A MATHEMATICAL MODEL FOR THE CLASS V FLEXTENSIONAL UNDERWATER ACOUSTIC TRANSDUCER

91

A Mathematical Model for the Class V Flextensional Underwater Acoustic Transducer

Technical Report No. 12

Submitted to

Office of Naval Research
Acoustic Programs
Code 468

Contract Nonr 486(11)

Ralph A. Nelson, Jr.
Principal Investigator

L. H. Royster
Project Director

North Carolina State University

at Raleigh

January 1970

Abstract

The purpose of this investigation is to develop a mathematical model for the Class V flextensional underwater acoustic transducer.

The transducer is approximated through the consideration of three distinct problems. The problem of a thin piezoelectric disk with an arbitrary impedance on its edge is solved in terms of Bessel functions. The shell vibration problem is solved using a finite difference model to approximate the shell. The acoustic radiation problem is solved by obtaining the source density distribution for a system of quadrilaterals representing the transducer. With the source density of each quadrilateral, the near and far field pressures and velocities can be found. Utilizing these three components, a model is then constructed for the transducer.

A comparison of the results from the mathematical model with those obtained from experiments is made in order to validate the model.

Acknowledgement

This work was sponsored by the Office of Naval Research, Acoustics Programs, Contract NONR 486(11).

TABLE OF CONTENTS

TABLE OF CONTENTS (continued)

LIST OF TABLES

LIST OF FIGURES

1. INTRODUCTION

In general, the various flextensional designs can be placed in one of five different classes [2]. The purpose of this investigation is to develop a mathematical model for the Class V flextensional underwater acoustic transducer. A picture of a Class V transducer is shown in Figure 1.1 and a typical sketch in Figure 1.2. The Class V flextensional transducer design was originally proposed as having possible applications as a sonobuoy transducer.

As shown in Figure 1.2, a Class V design consists of two shallow spherical shells bonded at the common boundary by an epoxy cement to the edge of a thin piezoelectric disk. The piezoelectric disk is isolated electrically from the two shells by the removal of the electrodes from the region where there is contact between the disk and the shells. Sufficient epoxy is applied so as to firmly attach each of the shells to the disk. Two small holes are drilled through the shells and serve as entrances for the electrical leads of the disk.

To attain the stated objective, one develops a mathematical model for each of the important components of the system. Then, combining them in a manner similar to that used by Royster [21], one obtains an approximate working model for the complete system. The model is then programmed on the IBM 360-75 computer, and an evaluation is made by comparing experimental[1] and predicted results.

---

[1] Dahlke, H. E. and L. H. Royster. 1964. Unpublished notes on Shallow Shell Transducer. North American Aviation, Inc., Columbus, Ohio.

FIGURE 1.1 A CLASS V FLEXTENSIONAL UNDERWATER ACOUSTIC TRANSDUCER

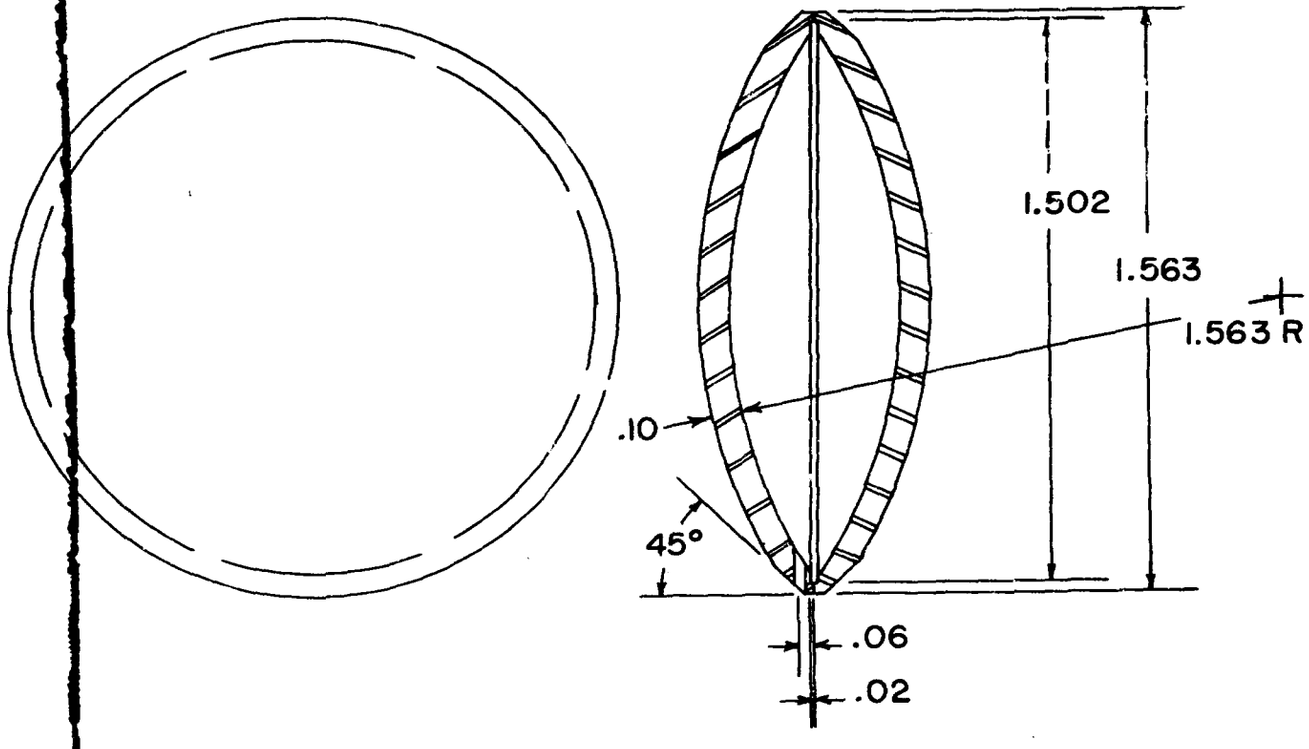

FIGURE 1.2 TYPICAL SKETCH OF A CLASS V TRANSDUCER

2. REVIEW OF LITERATURE

2.1 General

The development of detailed, complete mathematical models for the various classes of flextensional underwater acoustic transducers has been underway for about five years. Hence, the literature in this area is limited to only a few papers and technical reports. On the other hand, elements of the transducer problem, such as the thin piezoelectric disks, spherical caps, and acoustic radiation problems for different geometries have been studied extensively.

2.2 Mathematical Models of Flextensional Underwater Acoustic Transducers

The present state of the art of analytic models for flextensional underwater acoustic transducers is presented by Brigham and Royster [2]. They also classified the various flextensional transducer designs into five different classes. Presently, there are two analytic models, one complete and one partial, which have been presented. The complete model was presented by Royster [21] for the Class I transducer as shown in Figure 2.1. The partial model was presented by Boone and Royster [1] for the Class II transducer as shown in Figure 2.2. Both models use a finite difference model for the shell but differ in the manner by which the shell and stack are coupled and in the media in which they operate. The Class I model assumes that the shell vibrates independently of the stack and then solves the eigenvalue problem for the shell. On the other hand, the Class II model couples the electrode shorted stack to the shell through the edge segment equation of motion

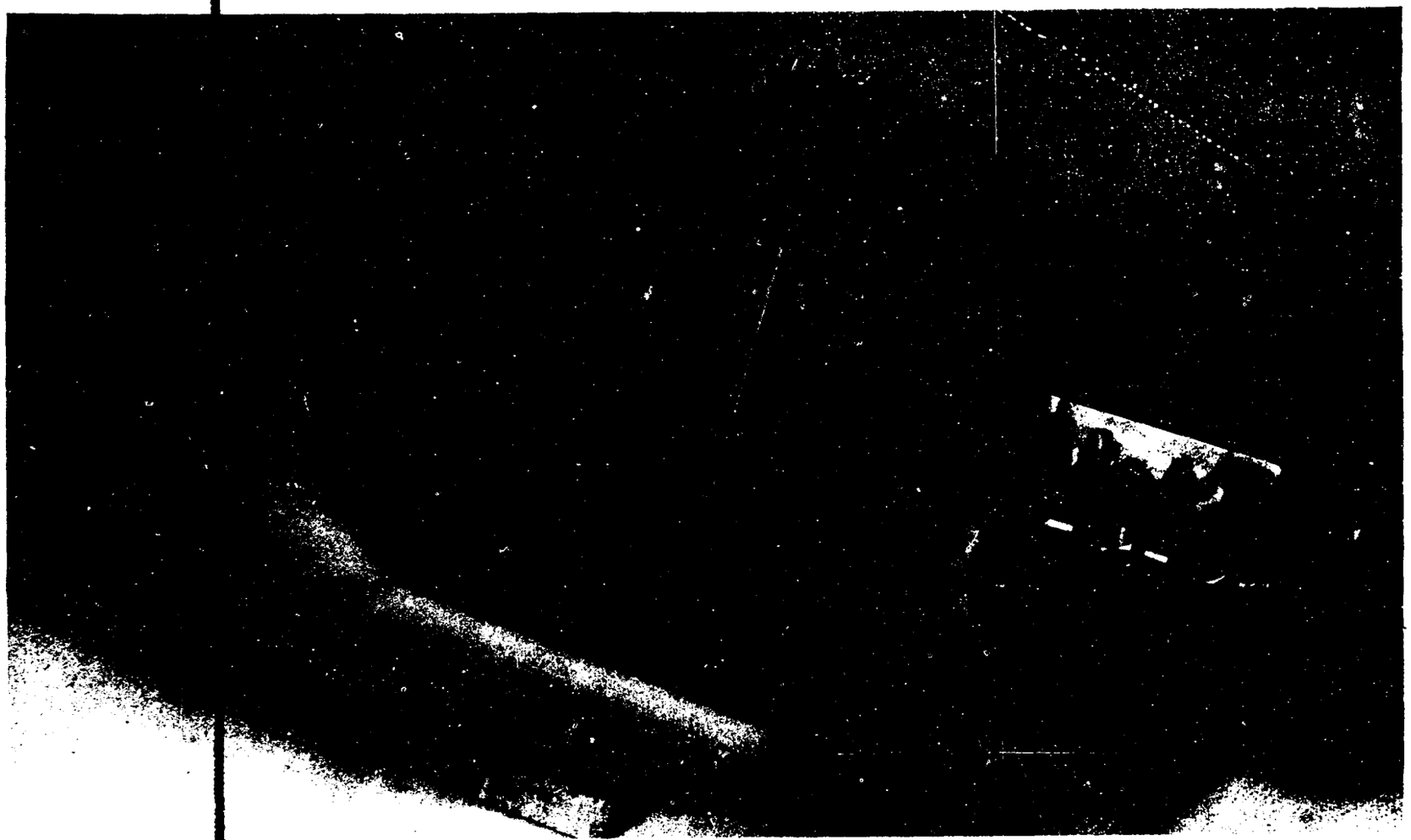

FIGURE 2.1 CLASS I FLEXTENSIONAL UNDERWATER ACOUSTIC TRANSDUCER

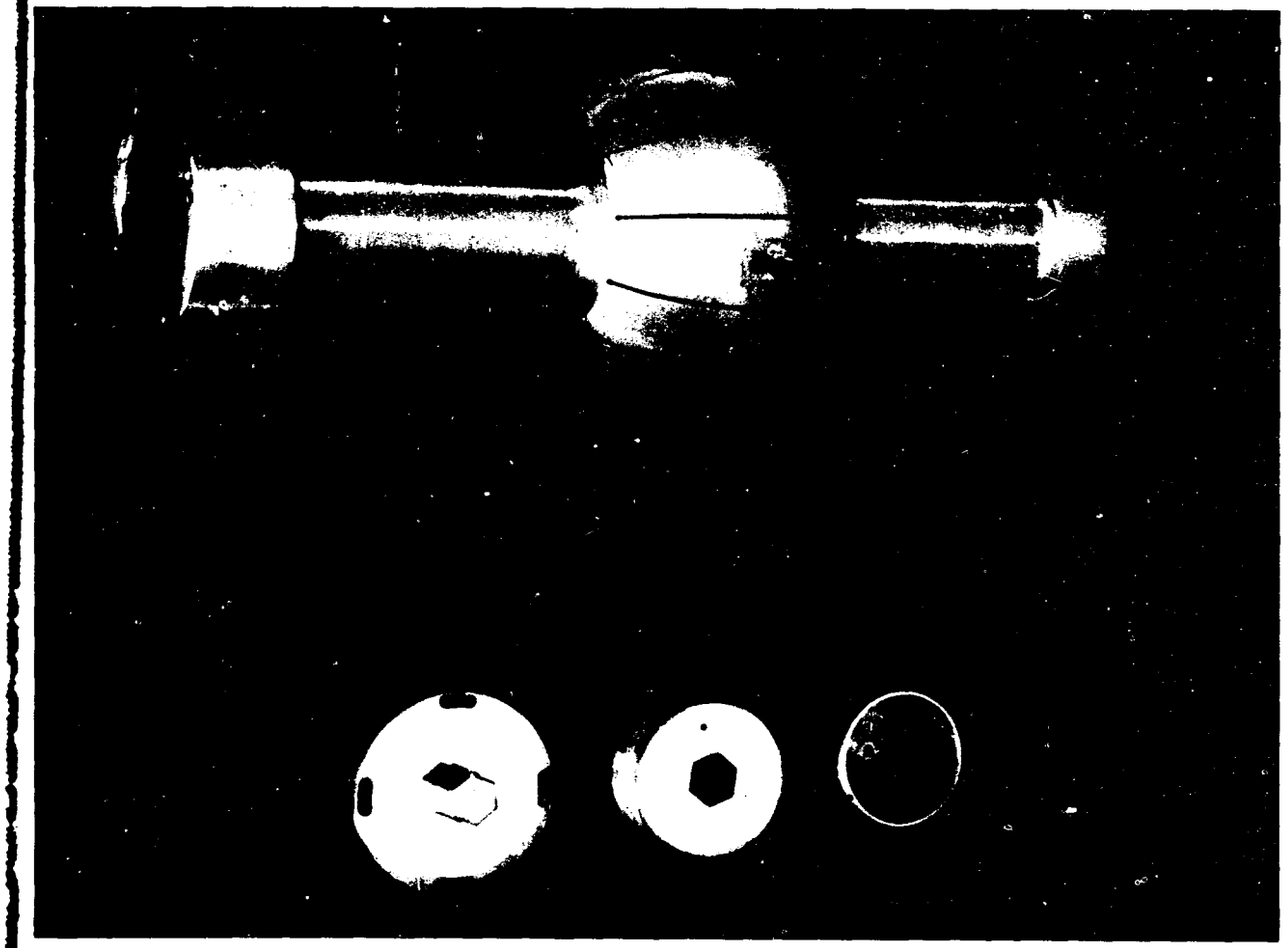

FIGURE 2.2 CLASS II FLEXTENSIONAL UNDERWATER ACOUSTIC TRANSDUCER

and then solves the eigenvalue problem. The Class I model can also operate in media which produce acoustic loads while the Class II model in its present state of development is limited to media which produce only negligible acoustic loads.

Presently, work is underway on discrete models for Classes II, III and IV at the Center for Acoustical Studies, and a continuous closed form solution for a Class IV oval is being developed by North American Aviation.

Since the mathematical model to be developed herein is for the Class V transducer, a review of the literature in the areas of thin piezoelectric disks, spherical caps, and acoustic radiation problems for three-dimensional bodies is of interest.

2.3 Thin Piezoelectric Disks

Three works in the literature are pertinent to an investigation of the vibration of a thin piezoelectric disk. The first of these is the vibration of a free, thin, electrostrictive disk by Mason [11]. Mason established the necessary system of equations and the assumptions and procedure needed to solve the problem. The resulting displacements differed from the elastic solution for a thin disk in that the material properties were measured in a constant electric field.

The second work by Tachibana [23], used Mason's procedure and solved the problem of a partially-plated, thin piezoelectric disk. Expressions for the displacement and electrical impedance were included in the results.

Building on the works of Mason and Tachibana, Nelson and Royster [14] obtained expressions for the electric impedance, resonant

frequencies, and dynamic electromechanical coupling coefficient for a thin piezoelectric disk with an arbitrary impedance on its boundary. The expressions were specialized for the case of a spring like boundary condition.

2.4 Spherical Caps

Langhaar [10] developed an expression for the strain energy in thin elastic shells. Special cases for the geometry were then considered, one of the cases being the sphere. From Langharr's strain energy expressions for a sphere, McDonald [12] obtained the equations of motion for a spherical cap with a clamped edge, using finite differences. These equations were then solved numerically for the eigenvalues and eigenvectors of the free undamped problem and were compared to other analytic results. The forced vibration problem was also solved for various loads.

Using the technique presented in his 1959 work, McDonald [13] then presented the equations of motion for free undamped vibration of a thin shell of revolution composed of an orthotropic material with variable elastic properties and thickness.

Nelson and Royster [15], utilizing the techniques presented in both papers by McDonald, derived the equations of motion for the guided-pinned and guided-clamped spherical cap. The results were then set up in matrix representation in order to obtain a numerical solution.

2.5 Acoustic Radiation

Three numerical techniques were considered as possible methods for obtaining the radiation field for the Class V flextensional transducer. This section will consist of a review of those techniques.

Chertock [3] developed a method for determining the radiation field of a vibrating body. In general, a Fredholm integral equation is solved numerically to give surface pressures. Then the special case of a surface of revolution with an arbitrary velocity distribution and frequency is described in detail.

Hess [8] developed a method of solving the radiation problem for an arbitrary three-dimensional body represented as a system of quadrilaterals. Specification of the geometry, normal surface velocities, and wave number leads to a set of linear algebraic equations which approximate an integral equation for the source density distribution. Solution of the system gives near and far field pressures as well as other information.

Schench [22] developed four different integral formulations for obtaining approximate solutions to the exterior steady-state acoustic radiation problem for an arbitrary surface whose normal velocity is specified. The fourth method, a Combined Helmholtz Integral Equation Formulation (CHIEF), overcomes numerical difficulties that arise for certain wave numbers.

The method chosen for use herein is that developed by Hess. This method was chosen due to its general approach to the body shape. The limitations of the method in the frequency range presented no problem since the fundamental mode of the Class V was well below the first "forbidden frequency."

3. DEVELOPMENT OF MATHEMATICAL MODEL

3.1 General

To develop a mathematical model for the Class V flextensional transducer, the model is divided into three sections. The first part is the vibration of a thin piezoelectric disk with an arbitrary impedance on its edge [14]. The second is the vibration of a spherical cap having a horizontally guided-pinned boundary condition [15]. The third section is the acoustic radiation problem due to the surface displacements on the shell.

The manner in which these three problems are joined depends on the assumptions made. Hence, discussion of this aspect of the overall transducer model will be delayed until after the three problems have been considered.

3.2 Equations of State

Both the equations of motion and the linear adiabatic equations of state for a piezoelectric material in a rectangular cartesian coordinate system were outlined by Royster [20] and the practical engineering limitations noted. Therefore, only the resulting equations, along with the assumptions made, will be noted here. In general, the notation used will also follow that outlined in the IRE (1949) publication [17].

The equations of motion arise out of the application of Newton's second law and are given by

$$T_{ij,j} + f_i = \rho \frac{d^2 u_i}{dt^2} \tag{3.1}$$

where T_{ij} is a symmetric tensor when body moments are neglected.

On the other hand, the equations of state cannot be so easily determined. First using the conservation of energy and then assuming that the dissipation of energy by the material is small compared to the rate of change of kinetic and potential energy, and that all processes are reversible, one can obtain

$$\dot{V}_p = T_{ij}\dot{S}_{ij} + E_i\dot{D}_i + \theta_T\dot{\sigma}^* \tag{3.2}$$

where $(\dot{})$ denotes differentiation with respect to time. From equation (3.2), it can then be assumed that

$$V_p = V_p(S_{ij}, D_i, \sigma^*) \ . \tag{3.3}$$

From equation (3.3), one can derive the two equations of state needed in the development of the mathematical model. In obtaining these equations of state, one must assume the following:

1) small deflection gradients (linear theory),

and

2) adiabatic process (no heat transferred).

These assumptions limit the transducer to low power applications. The resulting equations of state, which are commonly called the linear adiabatic equations of state, are given in rectangular cartesian tensor form by

$$S_{ij} = S^E_{ijk\ell}T_{k\ell} + d_{mij}E_m \tag{3.4}$$

and

$$D_n = d_{nk\ell}T_{k\ell} + \epsilon^T_{nm}E_m \ . \tag{3.5}$$

Equations (3.4) and (3.5) will be referred to simply as equations of state.

As shown in Figure 3.1, the coordinate system used for the thin piezoelectric disk is a cylindrical coordinate system. Use of the appropriate tensor transformations and material properties as shown in Appendix 7.1 results in the equations of state for cylindrical coordinates given by

$$
\begin{aligned}
S_{rr} &= S_{11}^{E} T_{rr} + S_{12}^{E}(T_{\theta\theta} + T_{zz}) + d_{31} E_z \\
S_{\theta\theta} &= S_{11}^{E} T_{\theta\theta} + S_{12}^{E}(T_{rr} + T_{zz}) + d_{31} E_z \\
S_{zz} &= S_{11}^{E} T_{zz} + S_{12}^{E}(T_{rr} + T_{\theta\theta}) \\
S_{r\theta} &= (S_{11}^{E} - S_{12}^{E}) T_{r\theta} \\
S_{rz} &= (S_{11}^{E} - S_{12}^{E}) T_{rz} \\
S_{\theta z} &= (S_{11}^{E} - S_{12}^{E}) T_{\theta z}
\end{aligned}
\tag{3.6}
$$

and

$$
D_z = d_{31}(T_{rr} + T_{\theta\theta}) + \epsilon_{33}^{T} E_z \, .
$$

3.3 Thin Piezoelectric Disk

The analytical results for a thin piezoelectric disk with an arbitrary impedance on its edge have been published [14]. The results presented did not discuss in depth the development of pertinent equations. Hence, this analytic effort will now be presented in detail in order to more clearly present the disk problem.

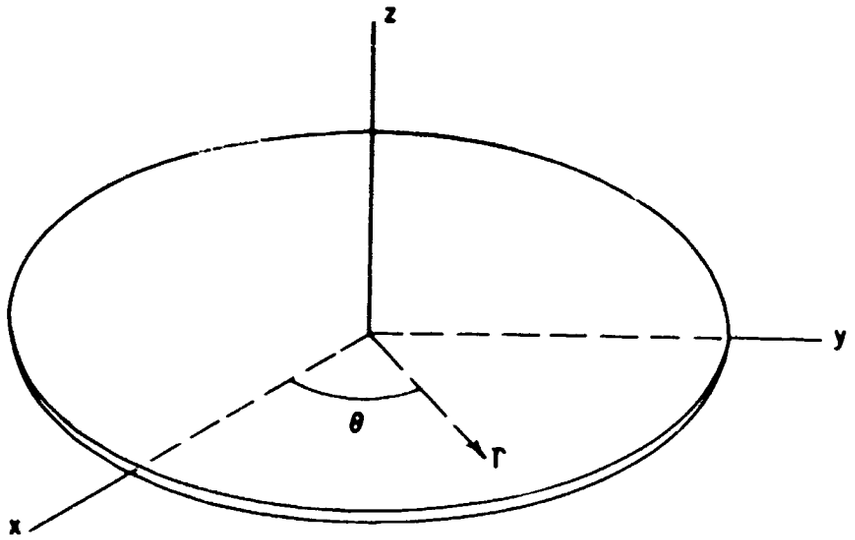

FIGURE 3.1 COORDINATE SYSTEM UTILIZED FOR THE PIEZOELECTRIC DISK

3.3.1 Electric Field and Piezoelectric Equations

The disk being considered is a thin circular disk with electrodes on the top and bottom as shown in Figure 3.2. The thickness of the disk, h_d, is much less than the radius of the disk, a_d, i.e., $h_d \ll a_d$.

In general, the displacements in cylindrical coordinates are denoted by

$$u_r = u_r(r, \theta, z, t)$$

$$u_\theta = u_\theta(r, \theta, z, t) \tag{3.7}$$

and

$$u_z = u_z(r, \theta, z, t) .$$

Now the motion will be assumed to be primarily radial. Therefore, there will be no displacement allowed in the θ direction, and all other displacements must be independent of θ. Also, the displacement in the radial direction will be required to be independent of z. Equation (3.7) can now be written as

$$u_r = u_r(r, t)$$

$$u_z = u_z(r, z, t) \tag{3.8}$$

and

$$u_\theta = 0 .$$

The stresses on a cylindrical element are shown in Figure 3.3. The bottom and top of the disk are free surfaces. Hence, since the

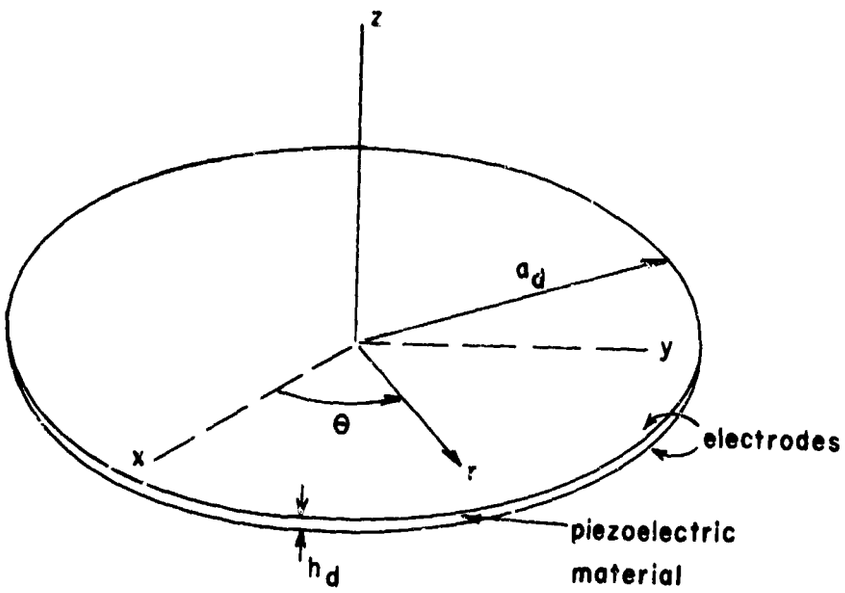

FIGURE 3.2 PIEZOELECTRIC DISK

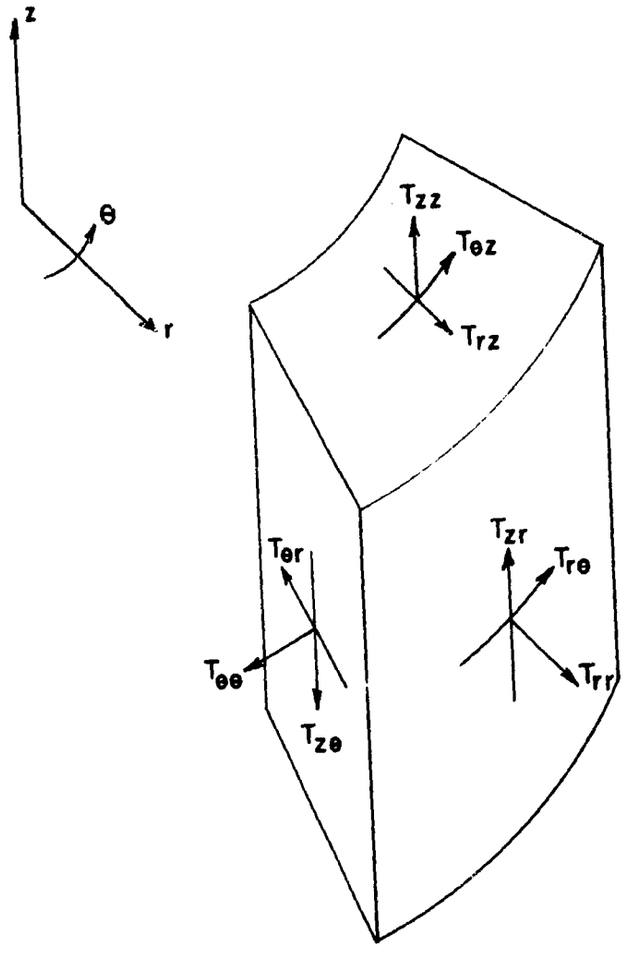

FIGURE 3.3 STRESSES ON A CYLINDRICAL ELEMENT OF VOLUME

disk is thin, one can assume that

$$T_{rz} = T_{\theta z} = T_{zz} = 0 \ . \tag{3.9}$$

The strain-displacement relations for cylindrical coordinates are given by Fung [5] to be

$$\begin{aligned} S_{rr} &= \frac{\partial u_r}{\partial r} , & S_{\theta\theta} &= \frac{1}{r}\frac{\partial u_\theta}{\partial \theta} + \frac{u_r}{r} , \\ S_{zz} &= \frac{\partial u_z}{\partial z} , & 2S_{r\theta} &= \frac{\partial u_\theta}{\partial r} - \frac{u_\theta}{r} + \frac{1}{r}\frac{\partial u_r}{\partial \theta} , \\ 2S_{rz} &= \frac{\partial u_r}{\partial z} + \frac{\partial u_z}{\partial r} , & 2S_{\theta z} &= \frac{1}{r}\frac{\partial u_z}{\partial \theta} + \frac{\partial u_\theta}{\partial z} \ . \end{aligned} \tag{3.10}$$

Substitution of equation (3.8) in equations (3.10) yields

$$\begin{aligned} S_{rr} &= \frac{\partial u_r}{\partial r} , & S_{\theta\theta} &= \frac{u_r}{r} , & S_{zz} &= \frac{\partial u_z}{\partial z} , \\ 2S_{rz} &= \frac{\partial u_z}{\partial r} , & \text{and} \quad S_{r\theta} &= S_{\theta z} = 0 \ . \end{aligned} \tag{3.11}$$

The equilibrium equations in cylindrical coordinates, which can be obtained from equation (3.1) through the procedure outlined in Appendix 7.1, are given by

$$\begin{aligned} \rho\ddot{u}_r &= \frac{\partial T_{rr}}{\partial r} + \frac{1}{r}\frac{\partial T_{r\theta}}{\partial \theta} + \frac{\partial T_{rz}}{\partial z} + \frac{T_{rr} - T_{\theta\theta}}{r} \\ \rho\ddot{u}_\theta &= \frac{\partial T_{r\theta}}{\partial r} + \frac{1}{r}\frac{\partial T_{\theta\theta}}{\partial \theta} + \frac{\partial T_{\theta z}}{\partial z} + 2\frac{T_{r\theta}}{r} \\ \rho\ddot{u}_z &= \frac{\partial T_{rz}}{\partial r} + \frac{1}{r}\frac{\partial T_{\theta z}}{\partial \theta} + \frac{\partial T_{zz}}{\partial z} + \frac{T_{rz}}{r} \ . \end{aligned} \tag{3.12}$$

Using equation (3.9) in equations (3.12), one obtains

$$\rho\ddot{u}_{rr} = \frac{\partial T_{rr}}{\partial r} + \frac{1}{r}\frac{\partial T_{r\theta}}{\partial \theta} + \frac{T_{rr}-T_{\theta\theta}}{r} \tag{3.13}$$

$$0 = \frac{\partial T_{r\theta}}{\partial r} + \frac{1}{r}\frac{\partial T_{\theta\theta}}{\partial \theta} + 2\frac{T_{r\theta}}{r} \tag{3.14}$$

and

$$\ddot{u}_z = 0 \ . \tag{3.15}$$

If the piezoelectric material has an electrically conducting plating on its surface, then the electric displacement can be assumed to be constant across the thickness of the disk. Also, the potential at each point along the radius is the same; consequently, E_z is independent of r [11], i.e.

$$\frac{\partial E_z}{\partial r} = 0 \ . \tag{3.16}$$

Using the results given by equation (3.9) in the piezoelectric equations of state (3.6), one obtains

$$\begin{aligned} S_{rr} &= S_{11}^E T_{rr} + S_{12}^E T_{\theta\theta} + d_{31}E_z \\ S_{\theta\theta} &= S_{11}^E T_{\theta\theta} + S_{12}^E T_{rr} + d_{31}E_z \\ S_{zz} &= S_{12}^E (T_{rr} + T_{\theta\theta}) \\ S_{r\theta} &= (S_{11}^E - S_{12}^E) T_{r\theta} \\ S_{rz} &= S_{\theta z} = 0 \end{aligned} \tag{3.17}$$

and $$D_z = d_{31}(T_{rr} + T_{\theta\theta}) + \epsilon_{33}^T E_z \ .$$

From equations (3.11) and (3.17), one can note that

$$S_{rz} = S_{\theta z} = S_{r\theta} = 0 \tag{3.18}$$

so that

$$\frac{\partial u_z}{\partial r} = 0 \tag{3.19}$$

and

$$T_{r\theta} = 0 \ . \tag{3.20}$$

One can now note, from equation (3.20) and the independence of the problem with respect to θ, that the equilibrium equation given by (3.14) is satisfied identically. From equations (3.8), (3.15), and (3.19), one observes that u_z is now restricted to being a function of z and a linear function of time. Therefore, it is now assumed that u_z is zero, so that equation (3.8) becomes

$$u_r = u_r(r,t) \tag{3.21}$$

and

$$u_\theta = u_z = 0 \ .$$

The strain-displacement equations given by (3.11) are reduced to

$$S_{rr} = \frac{\partial u_r}{\partial r} \qquad \text{and} \qquad S_{\theta\theta} = \frac{u_r}{r} \ . \tag{3.22}$$

The equilibrium equations become

$$\rho \ddot{u}_r = \frac{\partial T_{rr}}{\partial r} + \frac{T_{rr} - T_{\theta\theta}}{r} \ . \tag{3.23}$$

From equations (3.17), the equations of state for the two-dimensional radial motion of the disk are given by

$$S_{rr} = S_{11}^{E} T_{rr} + S_{12}^{E} T_{\theta\theta} + d_{31} E_z \tag{3.24}$$

$$S_{\theta\theta} = S_{11}^{E} T_{\theta\theta} + S_{12}^{E} T_{rr} + d_{31} E_z \tag{3.25}$$

and

$$D_z = d_{31}(T_{rr} + T_{\theta\theta}) + \epsilon_{33}^{T} E_z \ . \tag{3.26}$$

3.3.2 Equation of Motion

In order to obtain the equation of motion, one must find, from equations (3.24) and (3.25), the stresses in terms of strain and electric field. From Mason [11], it is found that

$$\frac{1}{S_{11}^{E}} = Y^{E} \qquad \text{and} \qquad -\frac{S_{12}^{E}}{S_{11}^{E}} = \sigma \ . \tag{3.27}$$

Hence, equations (3.24) and (3.25) yield

$$T_{rr} = \frac{Y^{E}}{1-\sigma^2} (S_{rr} + \sigma S_{\theta\theta}) - d_{31} \frac{Y^{E}}{1-\sigma} E_z \tag{3.28}$$

and

$$T_{\theta\theta} = \frac{Y^{E}}{1-\sigma^2} (S_{\theta\theta} + \sigma S_{rr}) - d_{31} \frac{Y^{E}}{1-\sigma} E_z \ . \tag{3.29}$$

Substitution of equations (3.28) and (3.29) into equation (3.23) gives

$$\rho \ddot{u}_r = \frac{Y^{E}}{1-\sigma^2} \left(\frac{\partial^2 u_r}{\partial r^2} + \frac{1}{r} \frac{\partial u_r}{\partial r} - \frac{u_r}{r^2} \right) \ . \tag{3.30}$$

Equation (3.30) is the equation of motion for a thin piezoelectric disk. This is identical to the equation of motion for a thin elastic disk and electrostrictive disk [11], except for the fact that Young's modulus in this case is measured under a constant electric field condition. Equation (3.30) is also identical to that obtained by Tachibana [23], as it should be.

3.3.3 Boundary Conditions and Initial Conditions

The model developed herein is limited to steady state vibrations; therefore, initial conditions are not necessary. Thus, one assumes a steady state displacement represented by

$$u_r(r,t) = U_r(r)e^{j\omega t} . \tag{3.31}$$

The first boundary condition to be given for the disk applies to its center. Since the only motion allowed is radial, then the center must not move; therefore,

$$U_r\Big|_{r=o} = 0 . \tag{3.32}$$

On the edge of the disk, an arbitrary specific impedance is applied. Hence, from Figure 3.4 and the definition of specific impedance [9], one obtains

$$-\frac{T_{rr}\Big|_{r=a_d}}{j\omega u_r\Big|_{r=a_d}} = Z' = \Omega + j\Gamma . \tag{3.33}$$

The arbitrary impedance consists of a real (resistive) part and an imaginary (reactive) part.

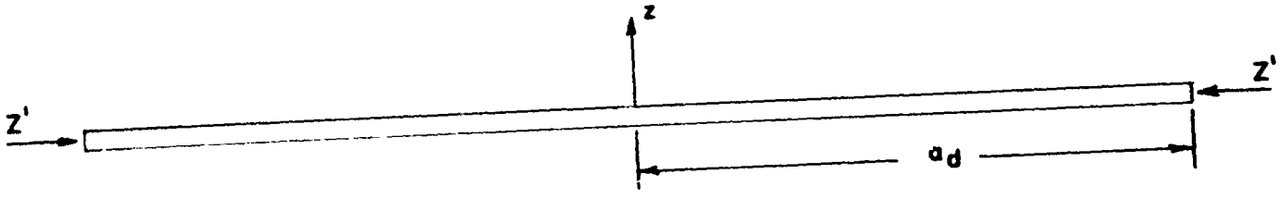

FIGURE 3.4 CROSS-SECTION OF DISK SHOWING ARBITRARY IMPEDANCE

3.3.4 Displacement, Stress, Electric Displacement and Impedance

To obtain the displacements of the disk, one first uses the steady state assumption given by equation (3.31) in the equation of motion given by equation (3.30) to obtain

$$x^2 \frac{d^2U_r}{dx^2} + x \frac{dU_r}{dx} + (x^2-1)U_r = 0 , \tag{3.34}$$

where

$$x = \frac{\omega r}{\nu} , \qquad x_d = \frac{\omega a_d}{\nu} , \tag{3.35}$$

and

$$\nu^2 = Y^E / \rho(1-\sigma^2) . \tag{3.36}$$

The parameter x will be called the dimensionless frequency parameter, while ν is the wave speed in the disk.

The solution of equation (3.34), which is a form of Bessel's equation, is given in Churchill [4]. Hence, one can write

$$U_r = AJ_1(x) + BY_1(x) , \tag{3.37}$$

where A and B are complex constants.

The boundary conditions given by equations (3.32) and (3.33) are now used. In order to satisfy (3.32), one must require B = 0 so that equation (3.37) becomes

$$U_r = AJ_1(x) . \tag{3.38}$$

Stresses, strains and the electrical field are also steady state forms.

For purposes of convenience, their exponentials will be dropped. Therefore, expressions and equations will be amplitude relations unless otherwise stated. Using equation (3.28) in (3.31) and the result from this substitution in equations (3.22), the steady state strains are found. The strains may then be used in equations (3.28) and (3.29) to obtain the steady state stresses. In particular, the radial stress is found to be

$$T_{rr} = \frac{Y^E A}{1-\sigma^2} \left[\frac{\omega}{v} J_o(x) - (1-\sigma) \frac{J_1(x)}{r} \right] - d_{31} \frac{Y^E}{1-\sigma} \frac{V_o}{h_d} \qquad (3.39)$$

where a steady state voltage of the form

$$V = V_o e^{j\omega t} \qquad (3.40)$$

has been assumed. Hence, using equations (3.31), (3.38) and (3.39) in the boundary condition given by equation (3.33), one can obtain the complex constant A so that the radial displacement, equation (3.38), becomes

$$U_r(r) = \frac{\gamma(\eta - j\delta)}{\eta^2 + \delta^2} \frac{J_1(x)}{\omega J_o(x_d)} \qquad (3.41)$$

where

$$\gamma = d_{31} \frac{Y^E}{1-\sigma} \frac{V_o}{h_d} \qquad (3.42)$$

$$\delta = \Omega \frac{J_1(x_d)}{J_o(x_d)} \qquad (3.43)$$

and

$$\eta = \frac{Y^E}{\nu(1-\sigma^2)} \left[1 - (1-\sigma) \frac{J_1(x_d)}{x_d J_o(x_d)} \right] - \Gamma \frac{J_1(x_d)}{J_o(x_d)} \quad . \tag{3.44}$$

From the procedure previously outlined, one determines the stresses in the disk to be

$$T_{rr} = \frac{Y^E}{\nu(1-\sigma^2)} \frac{\gamma(\eta - j\delta)}{\eta^2 + \delta^2} \left[\frac{J_o(x)}{J_o(x_d)} - (1-\sigma) \frac{J_1(x)}{(x) J_o(x_d)} \right]$$

$$- d_{31} \frac{Y^E}{1-\sigma} \frac{V_o}{d_h} \tag{3.45}$$

and

$$T_{\theta\theta} = \frac{Y^E}{\nu(1-\sigma^2)} \frac{\gamma(\eta - j\delta)}{\eta^2 + \delta^2} \left[\sigma \frac{J_o(x)}{J_o(x_d)} + (1-\sigma) \frac{J_1(x)}{(x) J_o(x_d)} \right]$$

$$- d_{31} \frac{Y^E}{1-\sigma} \frac{V_o}{h_d} \quad . \tag{3.46}$$

To obtain the steady state electric displacement, one simply inserts equations (3.45) and (3.46) into the piezoelectric equation of state for electric displacement given by (3.26), so that

$$D_z = \frac{Y^E d_{31}}{\nu(1-\sigma)} \frac{\gamma(\eta - j\delta)}{\eta^2 + \delta^2} \frac{J_o(x)}{J_o(x_d)} + \left[\epsilon_{33}^T - \frac{2d_{31}^2 Y^E}{1-\sigma} \right] \frac{V_o}{h_d} \quad . \tag{3.47}$$

Current is defined as the rate of flow of charge, i.e.

$$i = \frac{dQ}{dt} \quad . \tag{3.48}$$

Assuming a steady state charge, given by

$$Q = Q_T e^{j\omega t} , \tag{3.49}$$

equation (3.48) then gives

$$i = j\omega Q_T e^{j\omega t} = I_o e^{j\omega t} . \tag{3.50}$$

Electrical admittance, Y, and impedance, Z, are defined as follows:

$$Y = 1/Z = i/V . \tag{3.51}$$

Therefore, using equations (3.40) and (3.50) in (3.51), one obtains

$$Y = 1/Z = I_o/V_o = \frac{j\omega Q_T}{V_o} . \tag{3.52}$$

The total charge on the electrodes can be found by integrating the charge per unit area, D_z, over the surface of the electrode. One then has

$$Q_T = \int_o^{a_d} \int_o^{2\pi} D_z r \, dr \, d\theta . \tag{3.53}$$

From equation (3.47), one can note that $D_z = D_z(r)$ so that equation (2.53) becomes

$$Q_T = 2\pi \int_o^{a_d} D_z r \, dr . \tag{3.54}$$

Using equation (3.47) in (3.54) and carrying out the integration, one finds the total electrical charge to be

$$Q_T = 2\pi a_d^2 \frac{Y^E d_{31}}{\nu(1-\sigma)} \frac{\gamma(\eta - j\delta)}{\eta^2 + \delta^2} \frac{J_1(x_d)}{x_d J_o(x_d)}$$

$$+ \pi a_d^2 (\epsilon_{33}^T - \frac{2d_{31}^2 Y^E}{1-\sigma}) \frac{V_o}{h_d} \quad . \tag{3.55}$$

Using equation (3.55) in (3.52), the electrical admittance is given by

$$Y = g + jb \ , \tag{3.56}$$

where

$$g = 2\pi\omega a_d^2 \frac{Y^E d_{31}}{V_o(1-\sigma)\nu} \frac{\gamma\delta}{\eta^2 + \delta^2} \frac{J_1(x_d)}{x_d J_o(x_d)}$$

$$b = 2\pi\omega a_d^2 \left[\frac{Y^E d_{31}}{V_o(1-\sigma)\nu} \frac{\gamma\eta}{\eta^2 + \delta^2} \frac{J_1(x_d)}{x_d J_o(x_d)} \right.$$

$$\left. + \frac{\epsilon_{33}^T}{2h_d} (1 - k_p^2) \right] \tag{3.57}$$

and

$$k_p^2 = \frac{2}{1-\sigma} k_{31}^2 = \frac{2}{1-\sigma} \frac{d_{31}^2 Y^E}{\epsilon_{33}^T} \tag{3.58}$$

which is the planar coupling coefficient as given in the IRE standards of 1958 [18]. From equations (3.51) and (3.56), the electrical impedance can be shown as

$$Z = \frac{g - jb}{g^2 + b^2} \quad . \tag{3.59}$$

3.4 Shell Vibrations

As stated previously, the vibration of a spherical cap having a horizontally guided-pinned boundary condition has been studied by Nelson and Royster [15]. Their work was presented in enough detail so that a basic review will be all that is presented here.

3.4.1 Strain Energy in a Sphere

From the results presented by Langhaar [10], the strain energy due to stretching and bending can be obtained. The strain energy due to stretching is given by

$$U_1 = \frac{\mu}{1-\sigma} \int_0^{2\pi} \int_0^{\bar{\theta}} \{ (u_\theta + w)^2 + \csc^2\theta(v_\varphi + u\cos\theta + w\sin\theta)^2 + 2\sigma \csc\theta(u_\theta + w)(v_\theta + u\cos\theta + w\sin\theta) + \frac{(1-\sigma)}{2}\csc^2\theta(u_\varphi + v_\theta\sin\theta - v\cos\theta)^2 \} h_s \sin\theta\, d\theta\, d\varphi \qquad (3.60)$$

and the strain energy due to bending by

$$U_2 = \frac{\mu}{12(1-\sigma)} \int_0^{2\pi} \int_0^{\bar{\theta}} \{ w_{\theta\theta}^2 + \csc^4\theta(w_\theta \sin\theta\cos\theta + w_{\varphi\varphi})^2 + 2\sigma\csc^2\theta(w_{\theta\theta})(w_\theta\sin\theta\cos\theta + w_{\varphi\varphi}) + 2(1-\sigma)\csc^2\theta(w_\varphi\cot\theta - w_{\theta\varphi})^2 \} / (h_s^3/a_s^2) \sin\theta\, d\theta\, d\varphi \qquad (3.61)$$

where $u_\theta = \frac{\partial u}{\partial \theta}$, etc. . . . The coordinates system used for the spherical cap is shown in Figure 3.5. The potential energy of the external forces, U_{ext}, can be readily found from Figure 3.5 to be

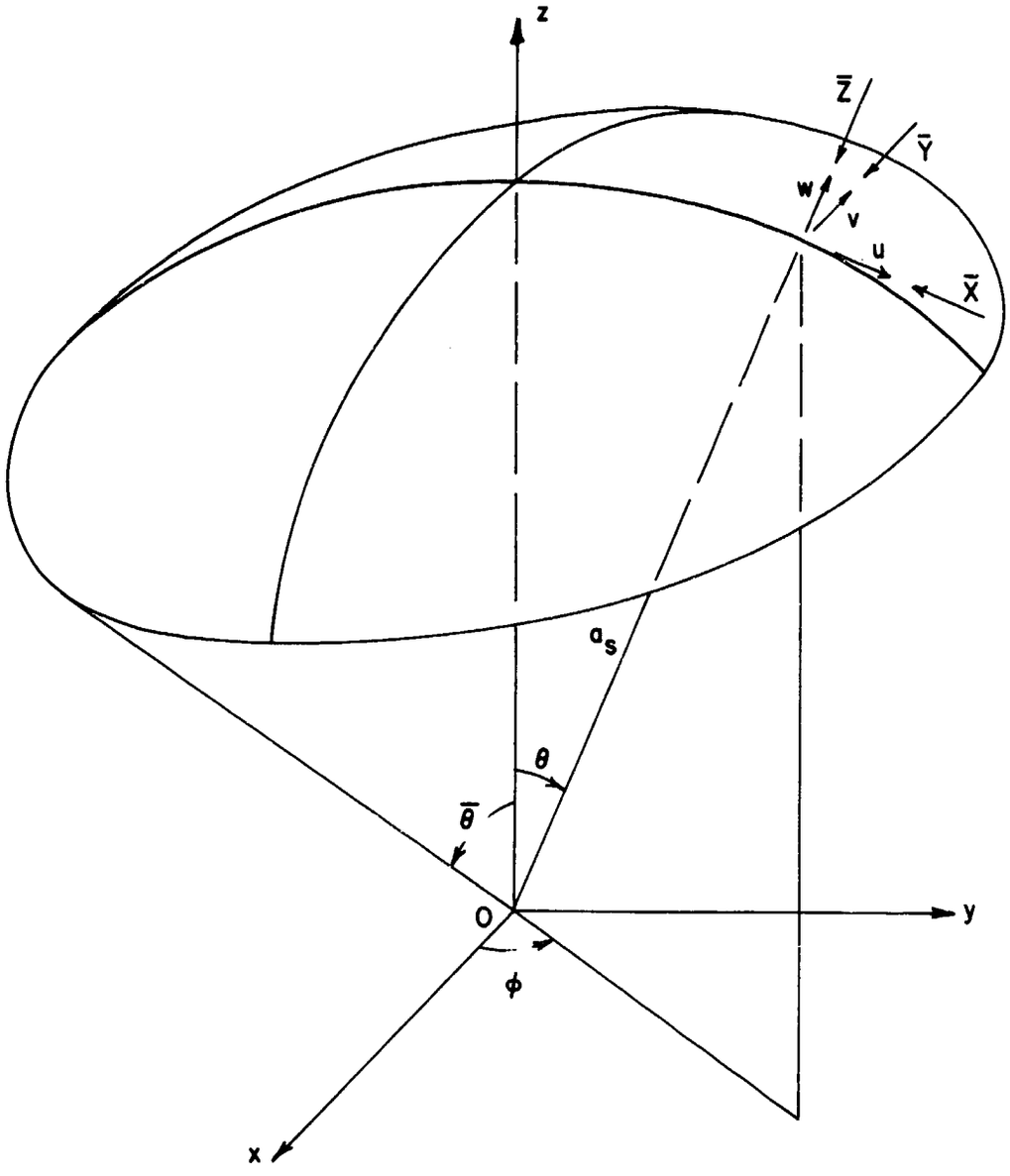

FIGURE 3.5 COORDINATE SYSTEM FOR THE SPHERICAL CAP

given as

$$U_{ext} = -a_s^2 \int_o^{2\pi} \int_o^{\bar{\theta}} (\bar{X}u + \bar{Y}v + \bar{Z}w) \sin\theta \, d\theta \, d\varphi \, . \tag{3.62}$$

Thus, the total strain energy V of the system is

$$V = U_1 + U_2 + U_{ext} \, . \tag{3.63}$$

Due to the symmetrical geometry of the transducer, one is only interested in rotationally symmetric vibrations. Requiring rotational symmetric vibrations and thus independence with respect to the circumferential variable, φ, equations (3.60), (3.61) and (3.62) reduce to

$$U_1 = \frac{2\pi\mu}{1-\sigma} \int_o^{\bar{\theta}} \{ (u_\theta + w)^2 + \csc^2\theta(u\cos\theta + w\sin\theta)^2 + 2\sigma \csc\theta(u_\theta + w)(u\cos\theta + w\sin\theta) \} h_s \sin\theta d\theta \, , \tag{3.64}$$

$$U_2 = \frac{2\pi\mu}{12(1-\sigma)a_s^2} \int_o^{\bar{\theta}} \{ w_{\theta\theta}^2 + \csc^4\theta(w_\theta \sin\theta\cos\theta)^2 + 2\sigma \csc^2\theta(w_{\theta\theta})(w_\theta \sin\theta\cos\theta) \} h_s^3 \sin\theta \, d\theta \, , \tag{3.65}$$

and

$$U_{ext} = -2\pi a_s^2 \int_o^{\bar{\theta}} (\bar{X}u + \bar{Z}w) \sin\theta \, d\theta \, . \tag{3.66}$$

3.4.2 Boundary Conditions

Two sets of boundary conditions are needed for the shell. The first set describes the crown point; the second set describes the lower edge of the shell, i.e. $\theta = \bar{\theta}$.

Rotationally symmetrical vibrations about the axis of revolution have been required for the shell. Therefore, the only possible motion at the crown point is one in which the crown is displaced in a radial direction. No tangential motion can accompany the radial motion, and from geometric considerations the slope remains zero. These requirements are expressed mathematically as

$$u\big|_{\theta=0} = 0 \tag{3.67}$$

and

$$\left.\frac{\partial w}{\partial \theta}\right|_{\theta=0} = 0 \, . \tag{3.68}$$

McDonald [13] adds to this set the requirement that

$$\left.\frac{\partial^3 w}{\partial \theta^3}\right|_{\theta=0} = 0 \, , \tag{3.69}$$

in order to insure a finite solution at the crown point.

It can be observed that the boundary conditions for the lower edge are somewhere between the guided-pinned and the guided-clamped cases. The degree to which the boundary conditions approach the clamped case depends upon the effect of the glued edges. For now, only the guided-pinned case will be considered. From Figure 3.6, the boundary conditions on the lower edge are

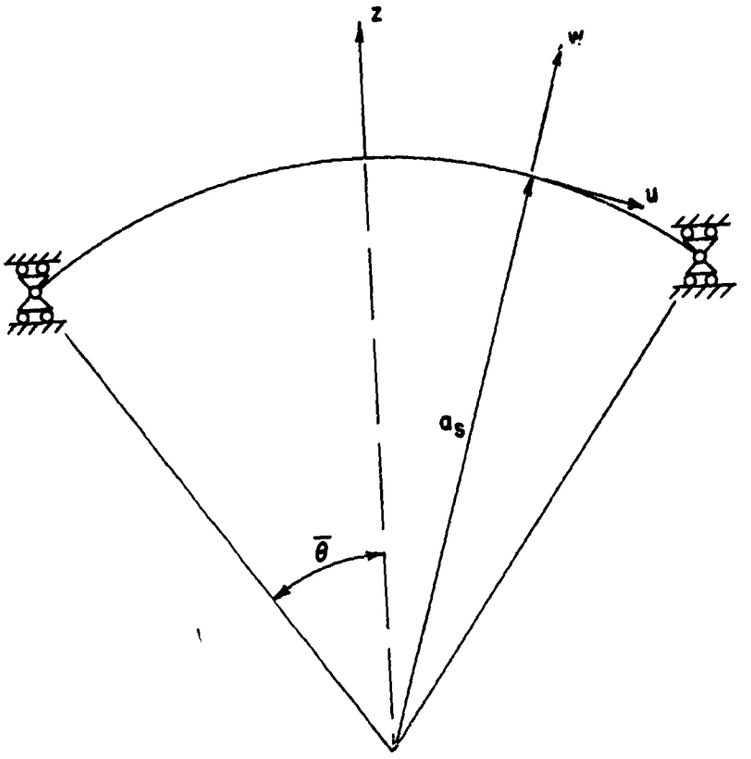

FIGURE 3.6 CROSS-SECTION VIEW OF THE GUIDED-PINNED BOUNDARY CONDITION

$$\text{bending moment at } (\theta = \bar{\theta}) = 0 , \tag{3.70}$$

and

$$\text{vertical displacement at } (\theta = \bar{\theta}) = 0 . \tag{3.71}$$

The boundary condition given by (3.70) will be discussed later when expressions for moments are written. The condition given by (3.71) can now be considered. Thus, from Figure 3.7, one can rewrite equation (3.71) as

$$w\big|_{\theta=\bar{\theta}} = u\big|_{\theta=\bar{\theta}} \tan \bar{\theta} . \tag{3.72}$$

To consider the guided-clamped case, one need only replace equation (3.70) with the requirement that the rate of change with respect to θ, at the lower edge of the shell, be zero.

3.4.3 Finite Difference Approximations for Derivatives

The finite difference approximations to be used in the construction of the model will now be considered. For the crown point, the following difference expressions will be used:

$$q_j' = \frac{\alpha}{2} (q_{j+1} - q_j) \tag{3.73}$$

$$q_j'' = \frac{\alpha^2}{4} (q_{j+1} - 2q_j + q_{j-1}) \tag{3.74}$$

and

$$q_j''' = \frac{\alpha^3}{8} (q_{j+2} - 3q_{j+1} + 3q_j - q_{j-1}) \tag{3.75}$$

where $j = 0$ for the crown point and $\Delta\theta$ is a half-angle increment so that

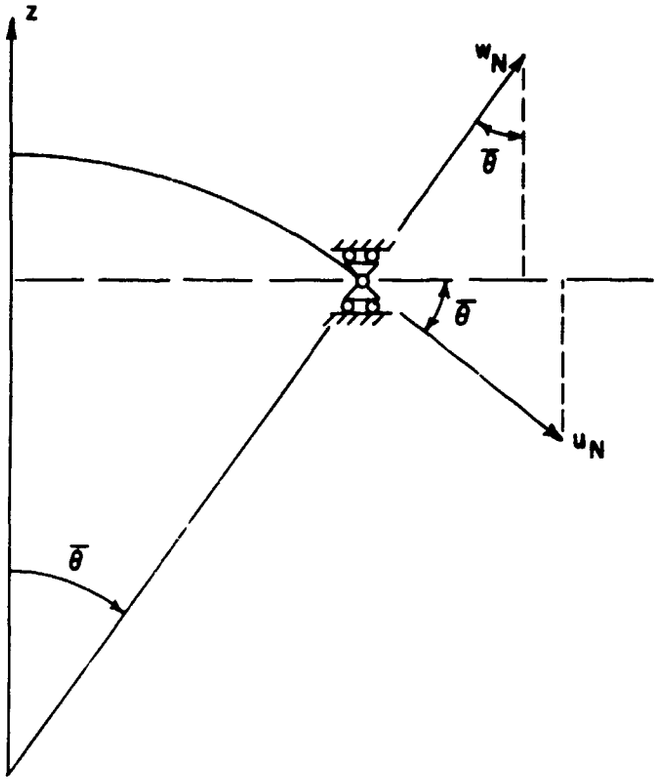

FIGURE 3.7 DISPLACEMENTS AT THE GUIDED-PINNED EDGE

$$\alpha = 1/\Delta\theta \quad . \tag{3.76}$$

For any interior point, the difference approximations used are

$$q_j' = \frac{\alpha}{2} (q_{j+1} - q_j) \tag{3.77}$$

and

$$q_j'' = \frac{\alpha^2}{4} (q_{j+1} - 2q_j + q_{j-1}) \quad . \tag{3.78}$$

For the lower edge, the difference approximations used are

$$q_j' = \frac{\alpha}{2} (q_j - q_{j-1}) \tag{3.79}$$

and

$$q_j'' = \frac{\alpha^2}{4} (q_{j+1} - 2q_j + q_{j-1}) \tag{3.80}$$

where j = N for the lower edge. The segment division and numbering can be seen more clearly in Figure 3.8.

3.4.4 Stress Resultants

The stress resultants in the shell can be determined from the displacements. This can be done because of the fact that the displacements in the shell are assumed known. From the displacements one can determine the strains. Then, by use of Hook's law for an isotropic media, one can determine stresses as a function of displacement. The stress resultants are then found by integrating the stresses across the thickness. McDonald [12], who references Vlasov [24], gives the following equations for the stress resultants:

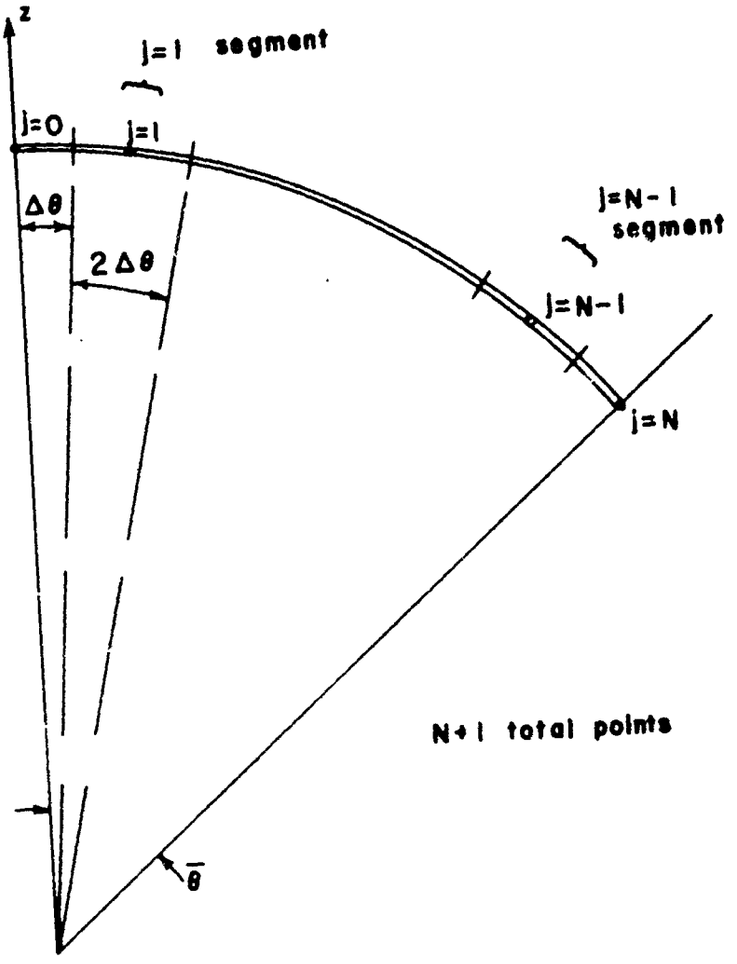

FIGURE 3.8 CROSS-SECTION VIEW SHOWING SEGMENT DIVISIONS AND NODE POINTS

$$M_\theta = D[w_{\theta\theta} + \sigma(w_{\varphi\varphi}\csc^2\theta + w_\theta \cot\theta)] \tag{3.81a}$$

$$M_\varphi = D[\sigma w_{\theta\theta} + (w_{\varphi\varphi}\csc^2\theta + w_\theta \cot\theta)] \tag{3.81b}$$

$$N_\theta = K[u_\theta + w + \sigma(u\cot\theta + v_\varphi \csc\theta + w)] \tag{3.81c}$$

$$N_\varphi = K[\sigma(u_\theta + w) + (u\cot\theta + v_\varphi \csc\theta + w)] \tag{3.81d}$$

where

$$D = \frac{Eh_s^3}{12(1-\sigma^2)}, \quad \text{and} \quad K = \frac{Eh_s}{12(1-\sigma^2)} . \tag{3.82}$$

The positive direction of the stress resultants is shown in Figure 3.9. For rotational symmetric vibrations, one can reduce equations (3.81) to the following:

$$M_\theta = D[w_{\theta\theta} + \sigma w_\theta \cot\theta] \tag{3.83a}$$

$$M_\varphi = D[\sigma w_{\theta\theta} + w_\theta \cot\theta] \tag{3.83b}$$

$$N_\theta = K[u_\theta + w + \sigma(u\cot\theta + w)] \tag{3.83c}$$

$$N_\varphi = K[\sigma(u_\theta + w) + u\cot\theta + w] . \tag{3.83d}$$

The stress resultants of the crown point can be written from equations (3.83) while noting the boundary conditions given by equations (3.67) and (3.68). Hence, one obtains

$$M_\theta\Big|_{\theta=0} = D\, w_{\theta\theta}\Big|_{\theta=0} \tag{3.84a}$$

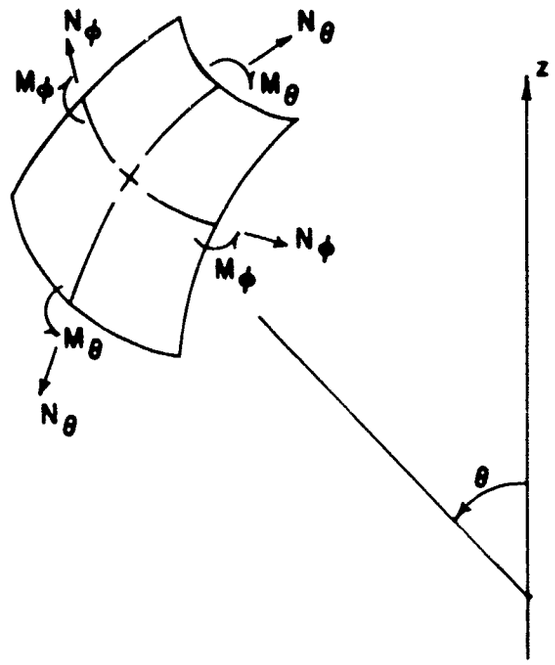

FIGURE 3.9 SIGN CONVENTION OF STRESS RESULTANTS

$$M_{\varphi}\Big|_{\theta=0} = D\sigma w_{\theta\theta}\Big|_{\theta=0} \tag{3.84b}$$

$$N_{\theta}\Big|_{\theta=0} = K[u_{\theta} + (1+\sigma)w]\Big|_{\theta=0} \tag{3.84c}$$

and

$$N_{\varphi}\Big|_{\theta=0} = K[\sigma u_{\theta} + (1+\sigma)w]\Big|_{\theta=0} . \tag{3.84d}$$

Using the finite difference approximations given by equations (3.73) and (3.74), one obtains the stress resultants in terms of difference expressions to be

$$(M_{\theta})_{j=o} = \frac{D\alpha^2}{4}(w_1 - 2w_0 + w_{-1}) \tag{3.85a}$$

$$(M_{\varphi})_{j=o} = \frac{D\sigma\alpha^2}{4}(w_1 - 2w_o + w_{-1}) \tag{3.85b}$$

$$(N_{\theta})_{j=o} = K[\frac{\alpha}{2}(u_1-u_o) + (1+\sigma)w_o] \tag{3.86a}$$

and

$$(N_{\varphi})_{j=o} = K[\frac{\sigma\alpha}{2}(u_1-u_o) + (1+\sigma)w_o] . \tag{3.86b}$$

Now the boundary condition given by equation (3.69) can be used in connection with equation (3.75) to obtain

$$w_{-1} = 3w_o - 3w_1 + w_2 . \tag{3.87}$$

Therefore, inserting equation (3.87) in (3.85) results in

$$(M_\theta)_{j=0} = \frac{D\alpha^2}{4}[w_o - 2w_1 + w_2] \tag{3.88a}$$

and

$$(M_\varphi)_{j=o} = \frac{D\sigma\alpha^2}{4}[w_o - 2w_1 + w_2] . \tag{3.88b}$$

For an interior point, the stress resultants on the k^{th} segment are found to be

$$(M_\theta)_{j=k} = \frac{D}{4}[\alpha^2 w_{k-1} - 2\alpha(\alpha + \sigma\cot\frac{2k}{\alpha})w_k + \alpha(\alpha + 2\sigma\cot\frac{2k}{\alpha})w_{k+1}] \tag{3.89a}$$

$$(M_\varphi)_{j=k} = \frac{D}{4}[\sigma\alpha^2 w_{k-1} - 2\alpha(\sigma\alpha + \cot\frac{2k}{\alpha})w_k + \alpha(\sigma\alpha + 2\cot\frac{2k}{\alpha})w_{k+1}] \tag{3.89b}$$

$$(N_\theta)_{j=k} = \frac{K}{2}[(2\sigma\cot\frac{2k}{\alpha} - \alpha)u_k + \alpha u_{k+1} + (1+\sigma)w_k] \tag{3.89c}$$

and

$$(N_\varphi)_{j=k} = \frac{K}{2}[(2\cot\frac{2k}{\alpha} - \alpha\sigma)u_k + \sigma\alpha u_{k+1} + (1+\sigma)w_k] . \tag{3.89d}$$

For the lower edge, i.e. $\theta = \bar{\theta}$, the stress resultants are given by

$$(M_\theta)_{j=N} = \frac{D}{4}[\alpha(\alpha - 2\sigma\cot\bar{\theta})w_{N-1} - 2\alpha(\alpha - \sigma\cot\bar{\theta})w_N + \alpha^2 w_{N+1}] \tag{3.90a}$$

$$(M_{\varphi})_{j=N} = \frac{D}{4}\left[\alpha(\alpha\sigma - 2\cot\bar{\theta})w_{N-1} - 2\alpha(\sigma\alpha - \cot\bar{\theta})w_N + \sigma\alpha^2 w_{N+1}\right] \quad (3.90b)$$

$$(N_{\theta})_{j=N} = \frac{K}{2}\left[-\alpha u_{N-1} + (\alpha + 2\sigma\cot\bar{\theta})u_N + 2(1+\sigma)w_N\right] \quad (3.90c)$$

and

$$(N_{\varphi})_{j=N} = \frac{K}{2}\left[-\sigma\alpha u_{N-1} + (\sigma\alpha + 2\cot\bar{\theta})u_N + 2(1+\sigma)w_N\right] . \quad (3.90d)$$

Hence, the boundary condition given by equation (3.70) can be used in connection with equation (3.90a) to obtain

$$w_{N+1} = \frac{2}{\alpha}(\alpha - \sigma\cot\bar{\theta})w_N - \frac{1}{\alpha}(\alpha - 2\sigma\cot\bar{\theta})w_{N-1} . \quad (3.91)$$

Therefore, using equations (3.91) and (3.72), where (3.72) can now be written as

$$w_N = u_N \tan\bar{\theta} \quad (3.92)$$

one can obtain the stress resultant on the lower edge.

3.4.5 Equations of Free Vibration

Lagrange's equation may be written as

$$\frac{d}{dt}\left(\frac{\partial L}{\partial \dot{q}_j}\right) - \frac{\partial L}{\partial q_j} = 0 \quad (3.93)$$

where L = T - V is the Lagrangian energy equal to the difference between the kinetic and potential energies, and where ($\dot{}$) denotes differentiation with respect to time, so that $\dot{q}_j$ represents the velocity of a generalized displacement. Hence, for a stationery

system, $T = 0$ and $V = V(q_o, q_1, \ldots, q_N)$ so that equation (3.93) becomes

$$\frac{\partial V}{\partial q_j} = 0 \ , \tag{3.94a}$$

where q in general represents u, v, and w or $3(N + 1)$ displacements for the discrete system being considered. For rotational symmetric considerations, at most $2(N + 1) - 1$ displacements remain.

The total potential energy of the discrete shell can be obtained by summing the energies on each segment, as now given by equation (3.63), so that

$$V = \sum_{j=o}^{N} \left[(U_1)_j + (U_2)_j + (U_{ext})_j \right] \ . \tag{3.94b}$$

The stretching and bending energies as given by equations (3.64) and (3.65) must now be obtained across each segment with appropriate consideration being given to the boundary conditions. Thus, for the boundary conditions to be considered here, one can obtain 2N simultaneous linear equations. In matrix notation this can be written as

$$\frac{2\pi\mu h_s}{1-\sigma} [S]\{q\} = \{p\} \tag{3.95}$$

where [S] is the 2N x 2N stiffness matrix,

{q} is the column vector of displacements,

{p} is the column vector of external forces,

and h_s has been assumed constant. The equations represented by (3.95) are for the spherical cap with a rotationally symmetric static load. To obtain the equations of free vibration for an undamped

system, one can replace the external forces with D'Alenbert inertia forces, expressed as

$$\bar{X} = -\rho h_s \ddot{u} \tag{3.96a}$$

and

$$\bar{Z} = -\rho h_s \ddot{w} \ . \tag{3.96b}$$

Hence, substituting equations (3.96) in equations (3.95) results in

$$\frac{2\pi\mu h_s}{1-\sigma} [S]\{q\} = -2\pi\rho h_s a_s^2 [M]\{\ddot{q}\} \ . \tag{3.97}$$

Assuming steady state motion given by

$$q(\theta,t) = q^*(\theta) e^{j\omega t} \ , \tag{3.98}$$

then equation (3.97) can be rewritten as

$$([S] - \lambda^2[M])\{q^*\} = 0 \tag{3.99}$$

where

$$\lambda^2 = 2\omega^2(1-\sigma^2)(\frac{\rho a_s^2}{E}) \ . \tag{3.100}$$

The stiffness and mass matrices denoted in equation (3.99) are not presented in detail here. As shown in Reference [15], they are found in a direct manner by integration of trigonometric quantities to obtain the equations of motion as presented in Appendix 7.2. These equations of motion are then written in matrix form resulting finally in equation (3.99).

3.5 Acoustic Radiation

The black box technique is used to solve the acoustic radiation portion of the problem. A computer program developed by Hess [8] is used. For any arbitrary three-dimensional body, one must input a surface geometry, surface normal velocity, and wave number to be considered. The input geometry is one that represents a system of quadrilaterals to approximate the surface of interest. The normal surface velocities are then the velocities of each quadrilateral making up the surface. The output is then made up in part by the surface pressures corresponding to each of the quadrilaterals and the far field pressures.

3.6 Model Construction

3.6.1 General

As discussed previously, the model consists of three basic parts. They are the disk, the shell, and the acoustic radiation problem. These three problems have now been discussed in sections 3.3, 3.4 and 3.5 respectively. The manner in which these problems are now connected depends upon what assumptions one chooses to make. The model construction will now proceed in the following order: shell, acoustic radiation loads, and disk. The assumptions made will be discussed at the point at which they are made and are basically the same as those used by Royster [21].

3.6.2 Shell Vibrations

3.6.2.1 Model Analysis. One can recall that the equations of motion for an undamped spherical cap undergoing free vibration were given by equation (3.99) as

$$([S] - \lambda^2[M])\{q^*\} = 0 \ . \tag{3.99}$$

This represents the spherical cap alone with guided pinned lower edge. The physical transducer, on the other hand, does not let the shell vibrate freely. The piezoelectric disk provides resistance to the free motion of the shell. Hence to solve the true problem, one must couple the disk to the shell before the free vibration problem is solved. However, if the disk adds little stiffness to the shell then one can assume that the solution of equations (3.99) for the eigenvector form without including the effects of the disk will be approximately equal to the solution with the disk consideration. Thus, making this assumption, one can solve the eigenvalue problem given by equation (3.99) by the techniques outlined by both Royster [20] and McDonald [13].

To obtain the equations of motion for the forced vibration problem, one considers equation (3.95) where both external forces and inertia forces are to be considered. Thus, instead of equations (3.96), one considers

$$\bar{X} = -\rho h_s \ddot{u} + X \tag{3.101a}$$

and

$$\bar{Z} = -\rho h_s \ddot{w} + Z \tag{3.101b}$$

where X and Z cannot contain inertia effects. Hence, using equations (3.101) in equations (3.95), one can obtain

$$\frac{2\pi\mu h_s}{1-\sigma}[S]\{q\} + 2\pi\rho a_s^2 h_s[M]\{\ddot{q}\} = 2\pi a_s^2\{p\} \tag{3.102}$$

where

$$\{q\} = \begin{bmatrix} u_1 \\ u_2 \\ \vdots \\ u_N \\ w_o \\ w_1 \\ \vdots \\ w_{N-1} \end{bmatrix} \quad \text{and} \quad \{p\} = \begin{bmatrix} \int_{1/\alpha}^{3/\alpha} X_1 \sin\theta\, d\theta \\ \vdots \\ \int_{\bar{\theta}-1/\alpha}^{\bar{\theta}} X_N \sin\theta\, d\theta \\ \int_{0}^{1/\alpha} Z_o \sin\theta\, d\theta \\ \vdots \\ \int_{\bar{\theta}-3/\alpha}^{\bar{\theta}-1/\alpha} Z_{N-1} \sin\theta\, d\theta \end{bmatrix}. \tag{3.103}$$

Now, using the eigenvectors of the free vibration problem as a basis, one can assume the vector for the solution of the forced vibration to be of the form

$$\{q\} = \sum_{r=1}^{N} b_r\{\varphi_r\} \tag{3.104}$$

where b_r is a scalar and is called the scalar modal participation factor while $\{\varphi_r\}$ is the eigenvector of the free vibration problem corresponding to the λ_r eigenvalue. Hence, using equation (3.104) in (3.102) gives

$$\frac{2\pi\mu h_s}{1-\sigma}[S]\sum_{r=1}^{N} b_r\{\varphi_r\} + 2\pi\rho a_s^2 h_s[M]\sum_{r=1}^{N}\ddot{b}_r\{\varphi_r\} = 2\pi a_s^2\{p\} \quad . \tag{3.105}$$

Premultiplying by $\{\varphi_s\}^T$ and use of orthogonality as can be noted from Reference [6] gives

$$\frac{2\pi\mu h_s}{1-\sigma}\{\varphi_r\}^T[S]\{\varphi_r\} + 2\pi\rho a_s^2 h_s\ddot{b}_r\{\varphi_r\}^T[M]\{\varphi_r\} = 2\pi a_s^2\{\varphi_r\}^T\{p\} \quad . \tag{3.106}$$

Now from the free vibration problem, one has

$$[S] = \lambda_r^2[M] \quad , \tag{3.107}$$

so that, noting equation (3.100), one can obtain from (3.106)

$$\ddot{b}_r + \omega_r^2 b_r = \frac{1}{\rho h_s}\frac{\{\varphi_r\}^T\{p\}}{\{\varphi_r\}^T[M]\{\varphi_r\}} \quad . \tag{3.108}$$

The steady state solution for (3.108) is easily obtained so that the steady state expression for (3.104) is given by

$$\{q\} = -\frac{e^{j\omega t}}{\rho h_s}\sum_{r=1}^{N}\frac{1}{\omega^2\left[1-\left(\frac{\omega_r}{\omega}\right)^2\right]}\frac{\{\varphi_r\}^T\{p^*\}}{R_r}\{\varphi_r\} \tag{3.109}$$

where

$$p = p^* e^{j\omega t} \qquad \text{and} \qquad R_r = \{\varphi_r\}^T[M]\{\varphi_r\} \quad . \tag{3.110}$$

3.6.2.2 Mobility and Impedance. As stated in section 3.6.2.1, the shell has been assumed to vibrate independent of the disk. Hence, the shell problem is solved and then coupled to the disk problem.

considered in section 3.3, through the arbitrary specific impedance applied to the edge of the disk. Thus, it now becomes necessary to obtain the impedance around the lower edge of the shell.

Mobility is defined as

$$\text{mobility} = \frac{\text{velocity}}{\text{force}}, \tag{3.111}$$

so that from Figure 3.10 one can obtain the mobility at the lower edge to be

$$M_N = \frac{\dot{u}_N}{F(2\pi a_s \sin\bar{\theta}\cos\bar{\theta})} \quad . \tag{3.112}$$

Likewise, one can obtain the specific mobility to be given by

$$M_N^* = \frac{\dot{u}_N a_s \sin\bar{\theta}\,[\sin\bar{\theta}\sin 1/\alpha - (1-\cos 1/\alpha)\cos\bar{\theta}]}{F\cos\bar{\theta}} \quad . \tag{3.113}$$

To obtain the velocity in the tangential direction, $\dot{u}_N$, needed for (3.112) and (3.113), one can obtain from equation (3.109) that

$$\{\dot{q}\} = -j\,\frac{e^{j\omega t}}{\rho h_s}\sum_{r=1}^{N}\frac{1}{\omega\left[1-\left(\frac{\omega_r}{\omega}\right)^2\right]}\,\frac{\{\varphi_r\}^T\{p^*\}}{R_r}\{\varphi_r\} \quad . \tag{3.114}$$

The N^{th} component of equation (3.114) then gives the needed velocity. Hence, the mobility or specific mobility for the edge of the shell can now be obtained. It should be noted that, with a knowledge of the free vibration problem and the forcing function, one need only consider the first couple of terms of equation (3.114) to obtain a value of mobility around the first resonant frequency.

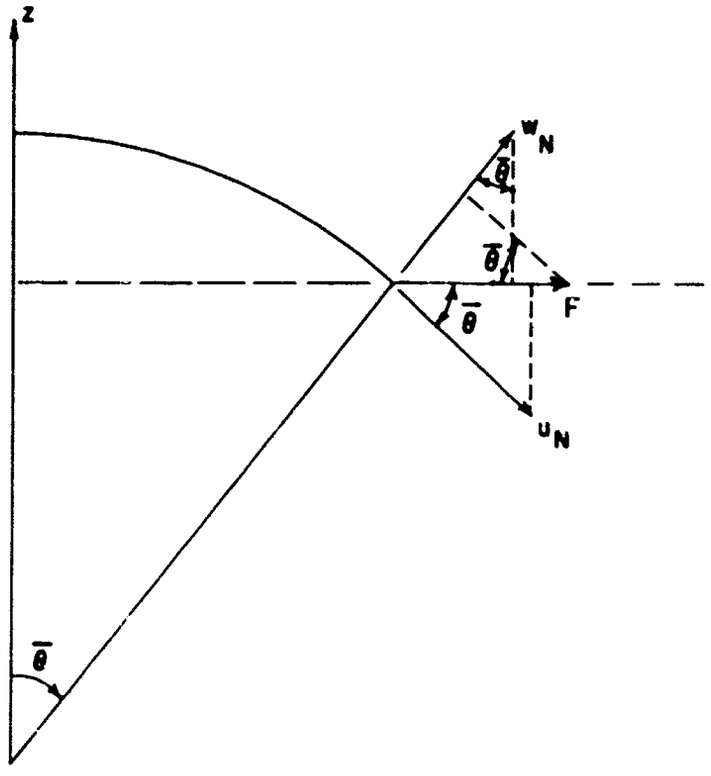

FIGURE 3.10 CROSS-SECTION VIEW OF DISPLACEMENT AND FORCE PER UNIT CIRCUMFERENCE AT THE LOWER EDGE

Impedance is the inverse of mobility. Therefore, from equations (3.112) and (3.113), one can determine that

$$Z_N = 1/M_N \tag{3.115}$$

and

$$Z_N^* = 1/M_N^* \quad . \tag{3.116}$$

3.6.3 Acoustic Radiation

For a given shell geometry, normal velocities, and wave number, Hess' program can be used to determine both the surface and far-field pressures. It should be noted that these values are per unit density of the fluid media. Two media will be considered in order to compare with the experimental results.

The first medium considered is air. Due to the density of the air, in comparison to that of the shell, one can neglect the resulting acoustic loads. Thus, the force vector in equation (3.103) reduces to only one component. Hence, the impedance of the shell can be found by using equations (3.112), (3.114) and (3.115).

The second medium to be considered is water. The forced vector now becomes complex. Assuming that the mode shape, including an external load, is not significantly changed from that of a vacuum, enabies one to greatly simplify the problem. The reactive part of the acoustic impedance can now be converted to an equivalent mass. This mass must then be added to the mass of the original structure, and the eigenvalue problem resolved for the necessary data required in Hess' numerical program. This iterative process can then be followed until

the system reaches equilibrium. Then, use of the conservation of energy in connection with the energy dissipated enables one to obtain the final resistive part of impedance to be applied to the disk.

3.6.4 Piezoelectric Disk

As discussed in section 3.6.3, with or without significant acoustic loads one can now obtain the resistive and reactive components of specific impedance, i.e. Ω and Γ, to be applied to the disk. Then, varying the excitation frequency of the disk, one can determine the electrical impedance of the particular transducer under consideration.

4. RESULTS

The mathematical model of the Class V flextensional underwater acoustic transducer as described in section 3.6 was programmed for evaluation on the IBM 360-75 computer [16]. Results for a particular geometry of the transducer can be found by defining the necessary physical parameters of the transducer.

For this investigation, experimental and mathematical model results are compared for a transducer similar to that shown in Figure 1.2. The thin piezoelectric disk has a diameter of 1.5 inches, a thickness of 0.04 inches, and the material is PZT-4 (PZT-4 is a Clevite Corporation trademark for a specific type of piezoelectric material). The aluminum spherical cap has a 1.563 inch inside radius and is 0.1 inches thick. The edge thickness of the spherical cap for each experimental transducer varies and is noted with its data. On the other hand, the mathematical model is restricted to constant thickness caps so that no variation in edge thickness is considered.

The experimental results[2] are presented in Table 4.1 and in Figures 4.1 and 4.2. The mathematical model results in air are presented in Figures 4.3 and 4.4. Figure 4.3 plots the magnitude of the electric impedance in ohms versus the driving frequency in kilohertz (khz) found using the mathematical model. Figure 4.4 shows both the analytic and experimental results for air in terms of decibels (db) versus driving frequency. The experimental results shown in Figure 4.4 are for transducer number 2.

---

[2] Ibid.

Table 4.1 Experimental results

Common geometric parameters of the transducer are listed below:

Piezoelectric disk: 1.5 inch diameter

0.04 inch thickness

PZT-4 material

Spherical caps: 1.563 inch inside radius

0.1 inch thickness

45° taper at edge to edge thickness

Transducer Number	Edge Thickness (inch)	Frequencies (khz)		
		Air		Water
		Resonance	Anti-resonance	
1	.015	21.8	22.6	12.5
2	.030	22.8	23.7	-

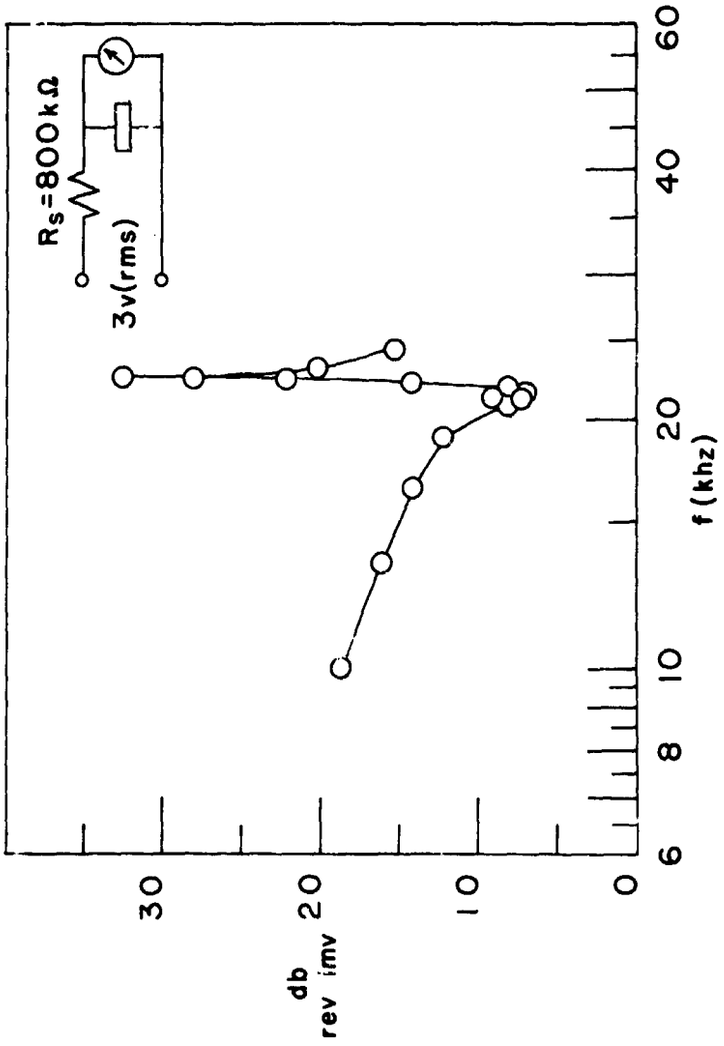

FIGURE 4.1 VOLTAGE ON TRANSDUCER #1 IN DB VERSUS DRIVING FREQUENCY

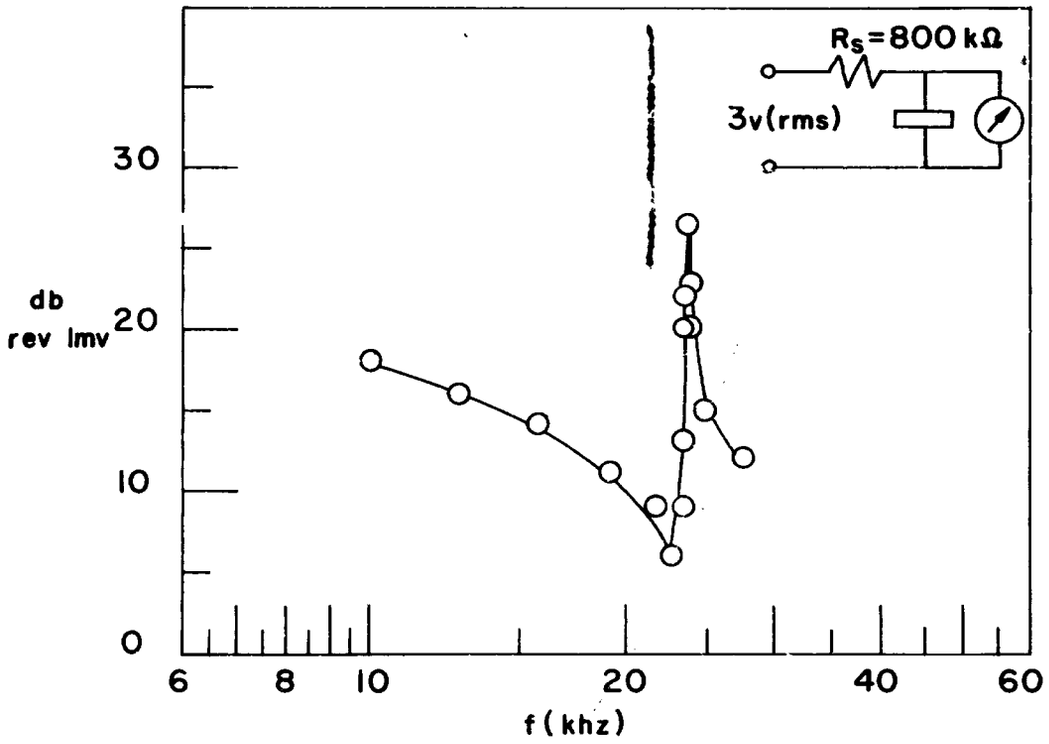

FIGURE 4.2 VOLTAGE ON TRANSDUCER #2 IN DB VERSUS DRIVING FREQUENCY

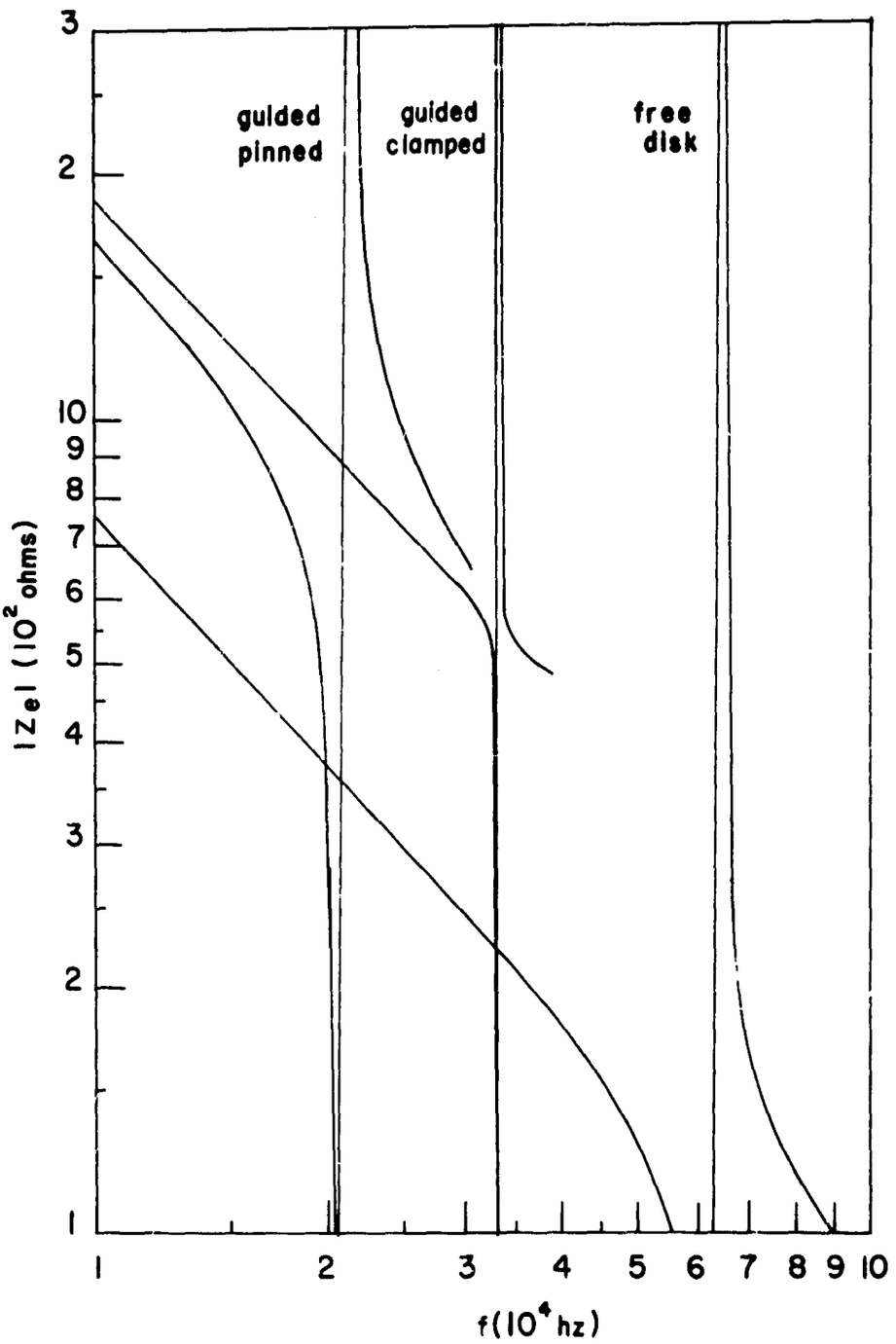

FIGURE 4.3 ELECTRICAL IMPEDANCE VERSUS DRIVING FREQUENCY FOR ANALYTIC MODEL IN AIR

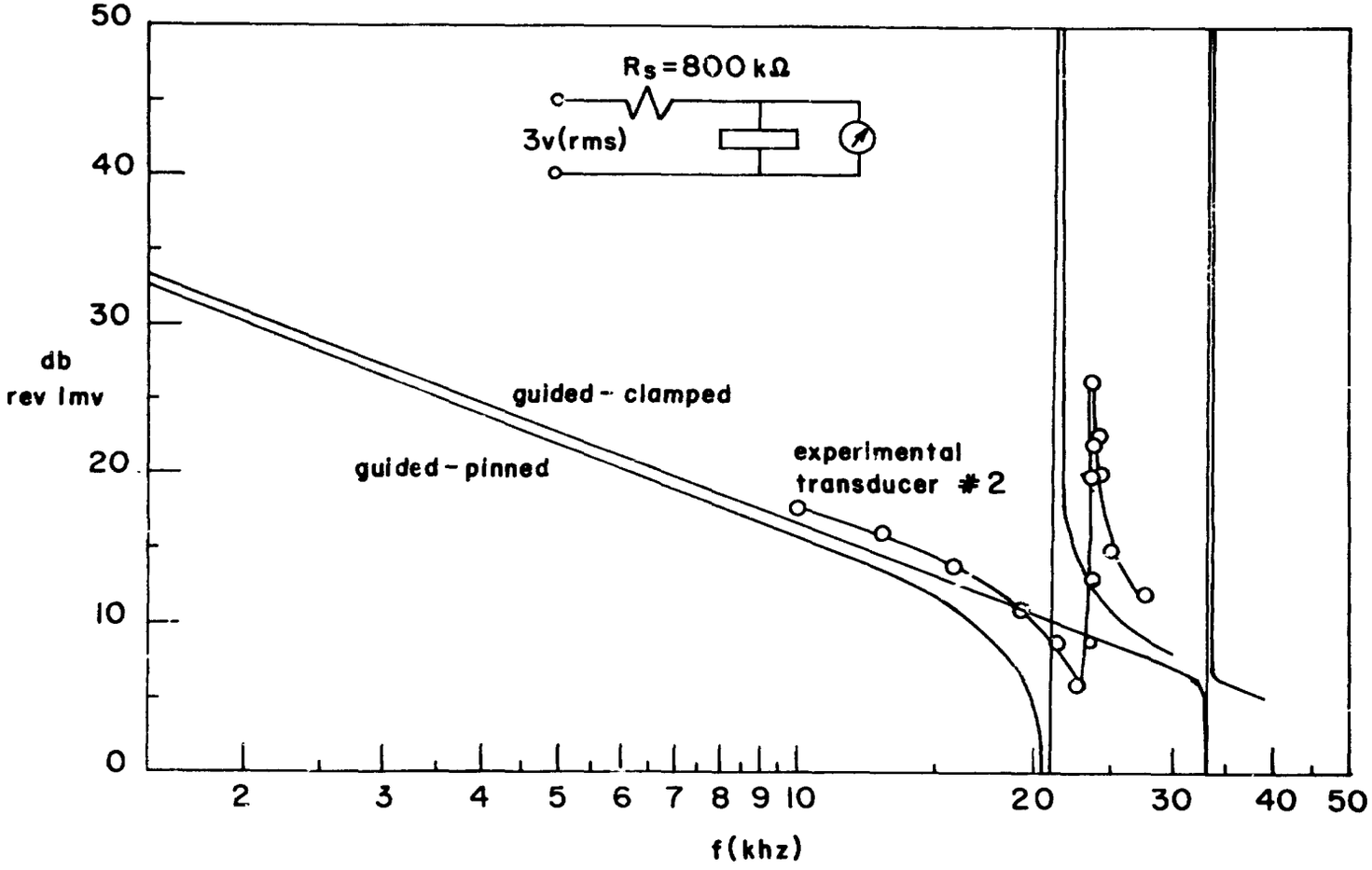

FIGURE 4.4 VOLTAGE ON TRANSDUCER IN DB VERSUS DRIVING FREQUENCY FOR ANALYTIC AND EXPERIMENTAL RESULTS IN AIR

In Figure 4.3, the analytic results of the free disk, the transducer model with a guided-pinned boundary condition, and the transducer model with a guided-clamped boundary condition are presented. These results show the disk to be dominated by the shell, as was assumed in section 3.6.2.1. The fundamental resonant frequencies for the guided-pinned and guided-clamped boundary conditions respectively are approximately 20.5 khz and 33.08 khz, while the anti-resonant frequencies are approximately 21.5 khz and 33.1 khz. Comparing these frequency bounds to the frequency results listed in Table 4.1, it is seen that the experimental frequency results do lie between the frequency bounds supplied by the mathematical model. It can also be seen that the guided-pinned model provides results much closer to the experimental results.

In Figure 4.4, the mathematical results in air for the two bounding boundary conditions are compared to the results of the experimental transducer number 2 for the electrical circuit shown. As noted above, the fundamental frequency of the experimental transducer is bounded by the mathematical results. However, away from resonance, the experimental results are not bounded by the results given by the two boundary conditions in the analytic model. This difference can be attributed to several possible causes. First, the inaccuracies inherent in the mathematical model itself. These inaccuracies can result from the uncoupling of the shell and disk, from the finite difference model used to approximate the shell, from assuming a constant thickness, and from the neglecting of the bond joints and their dissipation of energy. A second cause is the experimental

difficulty in obtaining measurements. Instrumentation inaccuracies are always present, and a variation of $\pm$ 1db is usually acceptable. Another point of interest is the dependence of the results on the series resistor, as shown by Royster [19]; therefore, a variation in the resistor, due to manufacturing tolerance, would produce a shift in the results.

To consider the transducer in water, acoustic loads can be obtained from the numerical program developed by Hess. The loads must be used in an iterative manner with the main program until the system converges tc the fundamental resonant frequency. In this case, four iterations were used. This required a total of 25 minutes of computer time. The resonant frequency of the analytic model was 11.65 khz, as compared to 12.5 khz of the experimental transducer number 1 in Table 4.1. This analytic case used the guided-pinned boundary condition, since the results in air showed the condition to give results nearer those found experimentally. A point of interest is found in that the shaved edge of the shell and the bond joint have opposing effects. While the degree to which each affects the results is not known, it might be possible for them to cancel each other out. This could be a prime factor in the good agreement between the guided-pinned analytic results and the experimental results.

In Figure 4.5, the magnitude of the electrical impedance of the transducer in water, with the guided-pinned boundary condition, is plotted against the driving frequency, while in Figure 4.6, the resistive part of the electric impedance for this case is plotted against the driving frequency. Since insufficient experimental

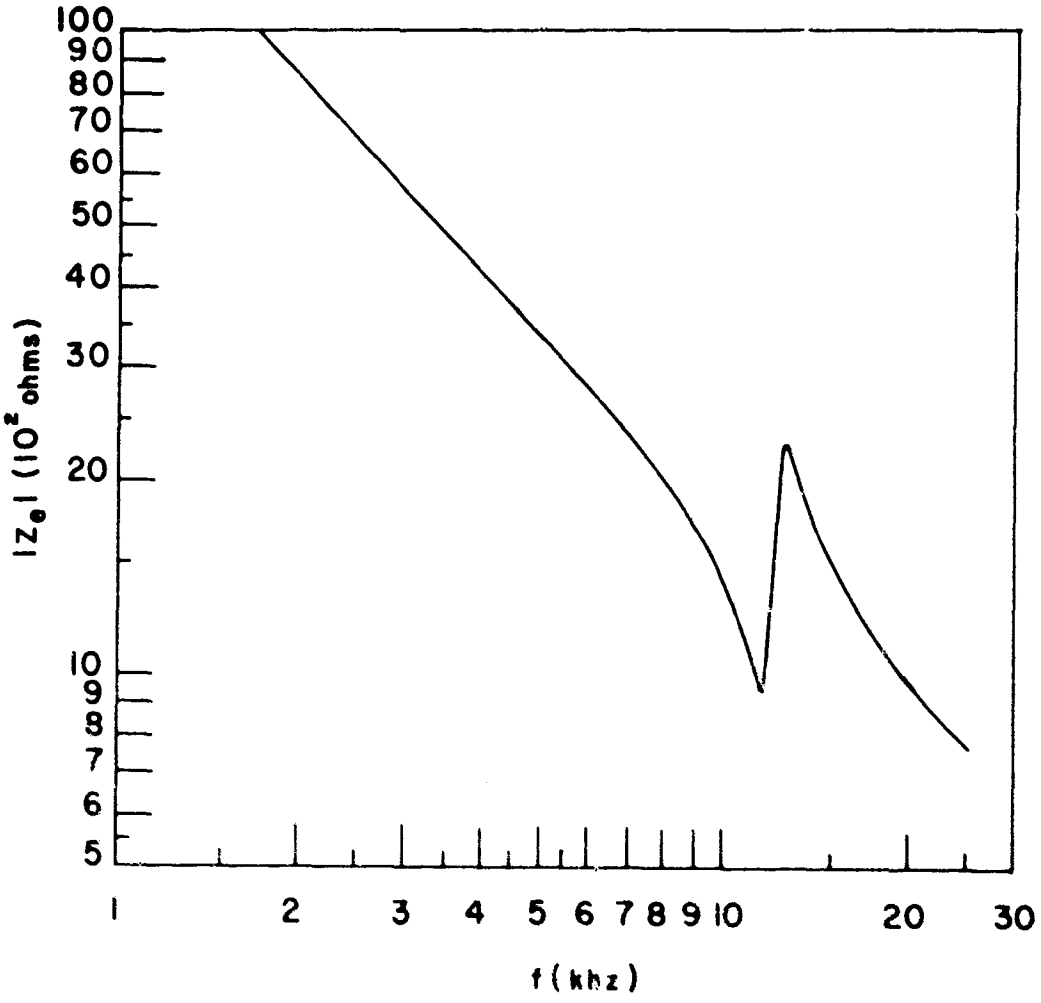

FIGURE 4.5 ELECTRIC IMPEDANCE OF THE TRANSDUCER IN WATER VERSUS DRIVING FREQUENCY

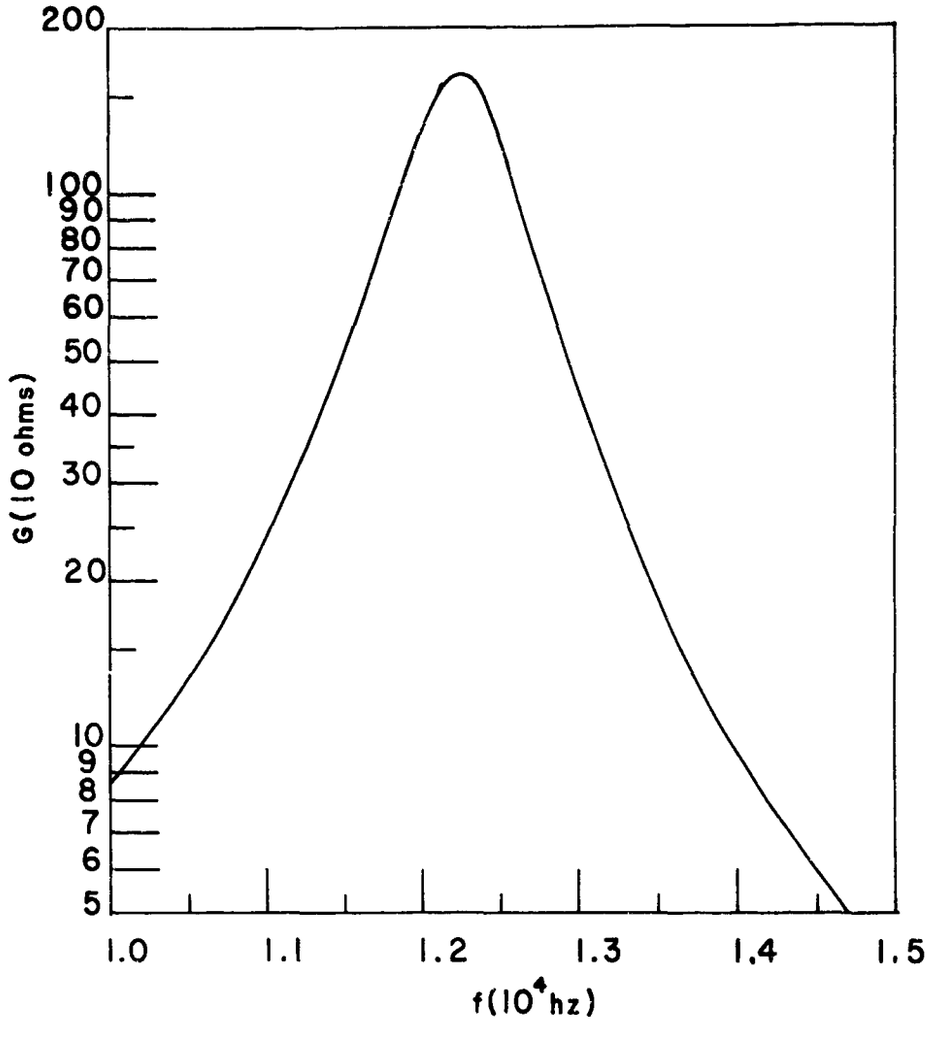

FIGURE 4.6 RESISTIVE PART OF THE ELECTRICAL IMPEDANCE IN WATER VERSUS THE DRIVING FREQUENCY

results are available to which these analytic results can be compared, a complete evaluation of this part of the model cannot be carried out at this time.

5. SUMMARY AND CONCLUSIONS

The fundamental resonant and anti-resonant frequencies in air of the experimental transducers were shown to be bound by the guided-pinned and guided-clamped results, with the guided-pinned condition giving results within approximately 5.9 percent of the experimental results. Therefore, using only the guided-pinned boundary condition in water, a fundamental resonant frequency of the mathematical model, which was only 6.8 percent lower than that found experimentally, was found. From these results, one can conclude that the mathematical model with the guided-pinned condition can be used to approximate the fundamental resonant frequencies.

In air, the electrical impedance of the transducer, found using the mathematical model developed herein, can be used in the electrical experimental circuit to read the voltage in db's across the transducer. These mathematical results are about 2 db's low for the guided-pinned case and 1 db low for the guided-clamped case as compared to the experimental results of transducer number 2.

In water, the electrical impedance and resistive portion of the electrical impedance can be obtained from the developed model, used in connection with the numerical program of Hess, for the acoustic loads. However, due to the lack of experimental data with respect to the electrical impedance, no statement can be made about the reliability of this portion of the model.

In conclusion, it can be said that the mathematical model developed herein gives results that compare well with existing experimental data. However, additional experimental data must be obtained

with respect to water loads before the validity of the analytic results for the loads presented herein can be verified.

6. LIST OF REFERENCES

1. Boone, J. N. and L. H. Royster. 1969. An approximate mathematical model for free vibrations of the class II flextensional underwater acoustic transducer model. Contract Nonr. 486(11), Technical Report No. 6, Department of Engineering Research, North Carolina State University at Raleigh, Raleigh, North Carolina.

2. Brigham, G. A. and L. H. Royster. 1969. Present status in the design of flextensional underwater acoustic transducers. J. Acoust. Soc. of America 46(1):92(A).

3. Chertock, G. 1964. Sound radiation from vibrating surfaces. J. Acoust. Soc. of America 36(7):1305-1313.

4. Churchill, R. V. 1963. Fourier Series and Boundary Value Problems. McGraw-Hill Book Co., Inc., New York, New York.

5. Fung, Y. C. 1965. Foundations of Solid Mechanics. Prentice-Hall, Inc., Englewood Cliffs, New Jersey.

6. Harris, C. M. and C. E. Crede. 1961. Shock and Vibration Handbook, Vol. 2. McGraw-Hill Book Co., Inc., New York, New York.

7. Hawkins, G. A. 1963. Multilinear Analysis for Students in Engineering and Science. John Wiley and Sons, Inc., New York, New York.

8. Hess, J. L. 1968. Calculation of acoustic fields about arbitrary three-dimensional bodies by a method of surface sources distributions based on certain wave number expansions. Report No. DAC 66901, McDonnel Douglas - Douglas Aircraft Corp., Long Beach, California.

9. Kinsler, L. E. and A. R. Frey. 1962. Fundamentals of Acoustics. John Wiley and Sons, Inc., New York, New York.

10. Langhaar, H. L. 1949. A strain-energy expression for thin elastic shells. Transactions of the American Society of Mechanical Engineers 16(2):183-189.

11. Mason, P. 1950. Piezoelectric Crystals and Their Application to Ultrasonics. D. Van Nostrand Co., Inc., New York, New York.

12. McDonald, D. 1959. A numerical analysis of the dynamic response of thin elastic spherical shells. Unpublished PhD thesis, Department of Civil Engineering, University of Illinois, Urbana, Illinois. University Microfilms, Ann Arbor, Michigan.

13. McDonald, D. 1965. Vibration characteristics of thin shells of revolution. TM54/20-14, Lockheed Missiles and Space Co., Huntsville, Alabama.

14. Nelson, R. A. and L. H. Royster. 1969. On the vibration of a thin piezoelectric disk with an arbitrary impedance on the boundary. J. Acoust. Soc. of America 46(3):829-830.

15. Nelson, R. A. and L. H. Royster. 1969. Development of a mathematical model for the class V flextensional underwater acoustic transducer shell. Contract Nonr. 486(11), Technical Report No. 8, Department of Engineering Research, North Carolina State University at Raleigh, Raleigh, North Carolina.

16. Nelson, R. A. and L. H. Royster. 1969. A fortran program for the class V flextensional underwater acoustic transducer. Contract Nonr. 486(11), Technical Report No. 11, Department of Engineering Research, North Carolina State University at Raleigh, Raleigh, North Carolina.

17. Proceedings of the IRE. 1949. Standards on piezoelectric crystals. IRE 37(12):1378-1395.

18. Proceedings of the IRE. 1958. IRE standards on piezoelectric crystals. IRE 46(4):764-777.

19. Royster, L. H. 1964. Piezo-electric projector research (summary of experimental evidence). Report NA64H-697, North American Aviation, Inc., Columbus, Ohio.

20. Royster, L. H. 1967. Investigation of the basic design principles of the flextensional underwater acoustic transducer. Contract Nonr. 486(11), Final Report, Department of Engineering Research, North Carolina State University at Raleigh, Raleigh, North Carolina.

21. Royster, L. H. 1969. The flextensional underwater acoustic transducer. J. Acoust. Soc. of America 45(3):671-682.

22. Schench, H. A. 1968. Improved integral formulation for acoustic radiation problems. J. Acoust. Soc. of America 44(1):41-58.

23. Tachibana, A. 1965. Partially plated thin-disk piezoelectric ceramic vibrators. Electron. Commun. 48(6):62-68.

24. Vlasov, V. S. 1951. Basic differential equations in general theory of elastic shells. N.A.C.A. Technical Memorandum 1241. Washington, D. C.

7. APPENDICES

7.1 Obtaining Cylindrical Equations of State from Cartesian Equations of State

As given by equations (3.4) and (3.5), the Cartesian tensor equations of state are given by

$$S_{ij} = S^{E}_{ijk\ell} T_{k\ell} + d_{mij} E_m \,, \tag{3.4}$$

and

$$D_n = d_{nk\ell} T_{k\ell} + \epsilon^{T}_{nm} E_m \,. \tag{3.5}$$

The tensor transformations, as given by Hawkins [7] for contravariant tensors of rank one and two respectively, are expressed as

$$E_m = \frac{\partial x_m}{\partial x'_n} E'_n \,, \tag{7.1}$$

and

$$T_{k\ell} = \frac{\partial x_k}{\partial x'_s} \frac{\partial x_\ell}{\partial x'_t} T'_{st} \,, \tag{7.2}$$

where E_m and $T_{k\ell}$ represent any contravariant tensors; x_m refers to the old coordinate system, and x'_n refers to the new coordinate system such that $x_m = x_m(x'_n)$.

Now, in order to transform equation (3.4) into curvilinear coordinates, one rewrites equation (7.2) as

$$S'_{st} = \frac{\partial x'_s}{\partial x_i} \frac{\partial x'_t}{\partial x_j} S_{ij} \,, \tag{7.3}$$

so that the curvilinear strains are in terms of the Cartesian strains.

Thus, using equation (3.4) in equation (7.3) gives

$$S'_{st} = \frac{\partial x'_s}{\partial x_i} \frac{\partial x'_t}{\partial x_j} S^E_{ijk\ell} T_{k\ell} + \frac{\partial x'_s}{\partial x_i} \frac{\partial x'_t}{\partial x_j} d_{mij} E_m , \tag{7.4}$$

which represents the curvilinear strains in terms of the Cartesian stress and electric field. Hence, using equations (7.1) and (7.2) in equation (7.4), one obtains the curvilinear equation of state corresponding to (3.4) to be

$$S'_{st} = \frac{\partial x'_s}{\partial x_i} \frac{\partial x'_t}{\partial x_j} S^E_{ijk\ell} \frac{\partial x_k}{\partial x'_m} \frac{\partial x_\ell}{\partial x'_n} T'_{mn} + \frac{\partial x'_s}{\partial x_i} \frac{\partial x'_t}{\partial x_j} d_{ijm} \frac{\partial x_m}{\partial x'_n} E'_n . \tag{7.5}$$

Similarly, the curvilinear equation corresponding to (3.5) is

$$D'_n = \frac{\partial x'_n}{\partial x_m} d_{mk\ell} \frac{\partial x_k}{\partial x'_s} \frac{\partial x_\ell}{\partial x'_t} T'_{st} + \frac{\partial x'_n}{\partial x_m} \varepsilon^T_{nm} \frac{\partial x_m}{\partial x'_s} E'_s . \tag{7.6}$$

Hence, equations (7.5) and (7.6) give the curvilinear tensor equations of state for a piezoelectric material.

One should note that, in general, the tensor components and physical components are the same only in a rectangular Cartesian system. Therefore, as shown in Fung [5], the tensor and physical components of a contravariant tensor of rank two are related by

$$\varepsilon_{ij} = \sqrt{g_{ii} g_{jj}}\, e_{ij} \quad \text{(no sum on i or j)} \tag{7.7}$$

where ε and e represent the physical and tensor components respectively and

$$g_{km} = \frac{\partial x_i}{\partial x'_k} \frac{\partial x_j}{\partial x'_m} \delta_{ij} . \tag{7.8}$$

To obtain the cylindrical equations of state, one simply has to follow the procedure outlined for the cylindrical-Cartesian transformation. The coordinate transformations can easily be obtained from Figure (3.1) to be

$$x = r\cos\theta\,, \quad y = r\sin\theta\,, \quad \text{and} \quad z = z\,, \tag{7.9}$$

or

$$r = \sqrt{x^2 + y^2}\,, \quad \theta = \tan^{-1}y/x\,, \quad \text{and} \quad z = z\,. \tag{7.10}$$

Hence, the resulting equations of state are given by

$$\begin{aligned}
S_{rr} &= S_{11}^E T_{rr} + S_{12}^E(T_{\theta\theta} + T_{zz}) + d_{31}E_z\,,\\
S_{\theta\theta} &= S_{11}^E T_{\theta\theta} + S_{12}^E(T_{rr} + T_{zz}) + d_{31}E_z\,,\\
S_{zz} &= S_{11}^E T_{zz} + S_{12}^E(T_{rr} + T_{\theta\theta})\,,\\
S_{r\theta} &= (S_{11}^E - S_{12}^E)\,T_{r\theta}\,,\\
S_{rz} &= (S_{11}^E - S_{12}^E)\,T_{rz}\,,\\
S_{\theta z} &= (S_{11}^E - S_{12}^E)\,T_{\theta z}\,,
\end{aligned} \tag{7.11}$$

and

$$D_z = d_{31}(T_{rr} + T_{\theta\theta}) + \epsilon_{33}^T E_z\,.$$

7.2 Equations of Motion for the Spherical Cap with Guided-Pinned Boundary Condition

As noted in section 3.4.5, the equations of motion for the boundary segments [illegible] se adjacent to them are affected by the

boundary conditions. Therefore, these equations must be derived for each segment and are, in general, different from the general interior equations. Defining the stiffness coefficient $S_{i\,j}^{k\,\ell}$, where ℓ_j refers to the displacement component by which the coefficient is multiplied, and k_i designates the particular equation from which the coefficient comes, one can obtain the following equations of motion:

j = 0, equation of motion with respect to w_0 (crown point)

$$(S_{0\,1}^{w\,u})u_1 + (S_{0\,0}^{w\,w})w_0 + (S_{0\,1}^{w\,w})w_1 + (S_{0\,2}^{w\,w})w_2 - (M_{0\,0}^{w\,w})w_0 = 0 , \quad (7.12)$$

j = 1, equation of motion with respect to u_1

$$(S_{1\,1}^{u\,u})u_1 + (S_{1\,2}^{u\,u})u_2 + (S_{1\,0}^{u\,w})w_0 + (S_{1\,1}^{u\,w})w_1 - (M_{1\,1}^{u\,u})u_1 = 0 , \quad (7.13)$$

equation of motion with respect to w_1

$$(S_{1\,1}^{w\,u})u_1 + (S_{1\,2}^{w\,u})u_2 + (S_{1\,0}^{w\,w})w_0 + (S_{1\,1}^{w\,w})w_1 + (S_{1\,2}^{w\,w})w_2 + (S_{1\,3}^{w\,w})w_3 - (M_{1\,1}^{w\,w})w_1 = 0 , \quad (7.14)$$

j = 2, equation of motion with respect to u_2 (or k = 2)

$$(S_{2\,1}^{u\,u})u_1 + (S_{2\,2}^{u\,u})u_2 + (S_{2\,3}^{u\,u})u_3 + (S_{2\,1}^{u\,w})w_1 + (S_{2\,2}^{u\,w})w_2 - (M_{2\,2}^{u\,u})u_2 = 0 , \quad (7.15)$$

equation of motion with respect to w_2

$$(S_{2\,2}^{w\,u})u_2 + (S_{2\,3}^{w\,u})u_3 + (S_{2\,0}^{w\,w})w_0 + (S_{2\,1}^{w\,w})w_1 + (S_{2\,2}^{w\,w})w_2 + (S_{2\,3}^{w\,w})w_3 + (S_{2\,4}^{w\,w})w_4 - (M_{2\,2}^{w\,w})w_2 = 0 , \quad (7.16)$$

$j = k, \quad k = 3,4,\ldots,N-4,N-3$

equations of motion with respect to u_k

$$(S^{uu}_{k\,k-1})u_{k-1} + (S^{uu}_{k\,k})u_k + (S^{uu}_{k\,k+1})u_{k+1} + (S^{uw}_{k\,k-1})w_{k-1}$$

$$+ (S^{uw}_{k\,k})w_k - (M^{uu}_{k\,k})u_k = 0 , \tag{7.17}$$

equations of motion with respect to w_k

$$(S^{wu}_{k\,k})u_k + (S^{wu}_{k\,k+1})u_{k+1} + (S^{ww}_{k\,k-2})w_{k-2} + (S^{ww}_{k\,k-1})w_{k-1}$$

$$+ (S^{ww}_{k\,k})w_k + (S^{ww}_{k\,k+1})w_{k+1} + (S^{ww}_{k\,k+2})w_{k+2} - (M^{ww}_{k\,k})w_k = 0 , \tag{7.18}$$

$j = N-2$, equation of motion with respect to $u_{N-2}(k = N-2)$

$$(S^{u\ u}_{N-2\,N-3})u_{N-3} + (S^{u\ u}_{N-2\,N-2})u_{N-2} + (S^{u\ u}_{N-2\,N-1})u_{N-1} + (S^{u\ w}_{N-2\,N-3})w_{N-3}$$

$$+ (S^{u\ w}_{N-2\,N-2})w_{N-2} - (M^{u\ u}_{N-2\,N-2})u_{N-2} = 0 , \tag{7.19}$$

equation of motion with respect to w_{N-2}

$$(S^{w\ u}_{N-2\,N-2})u_{N-2} + (S^{w\ u}_{N-2\,N-1})u_{N-1} + (S^{w\ u}_{N-2\,N})u_N + (S^{w\ w}_{N-2\,N-4})w_{N-4}$$

$$+(S^{w\ w}_{N-2\,N-3})w_{N-3} + (S^{w\ w}_{N-2\,N-2})w_{N-2} + (S^{w\ w}_{N-2\,N-1})w_{N-1}$$

$$- (M^{w\ w}_{N-2\,N-2})w_{N-2} = 0 , \tag{7.20}$$

$j = N-1$, equation of motion with respect to u_{N-1}

$$(S^{u\ u}_{N-1\,N-2})u_{N-2} + (S^{u\ u}_{N-1\,N-1})u_{N-1} + (S^{u\ u}_{N-1\,N})u_N + (S^{u\ w}_{N-1\,N-2})w_{N-2}$$

$$+ (S^{u\ w}_{N-1\,N-1})w_{N-1} - (M^{u\ u}_{N-1\,N-1})u_{N-1} = 0 , \tag{7.21}$$

equation of motion with respect to w_{N-1}

$$(S^{w\,u}_{N-1\,N-1})u_{N-1} + (S^{w\,u}_{N-1\,N})u_N + (S^{w\,w}_{N-1\,N-3})w_{N-3} + (S^{w\,w}_{N-1\,N-2})w_{N-2}$$
$$+ (S^{w\,w}_{N-1\,N-1})w_{N-1} - (M^{w\,w}_{N-1\,N-1})w_{N-1} = 0 , \qquad (7.22)$$

$j = N$, equation of motion with respect to u_N

$$(S^{u\,u}_{N\,N-1})u_{N-1} + (S^{u\,u}_{N\,N})u_N + (S^{u\,w}_{N\,N-2})w_{N-2} + (S^{u\,w}_{N\,N-1})w_{N-1}$$
$$- (M^{u\,u}_{N\,N})u_N = 0 . \qquad (7.23)$$

The stiffness coefficients of the stiffness matrix from the u_1 equation of motion are listed as follows:

$$S^{u\,u}_{1\,1} = \alpha^2\left[\frac{1-\cos 1/\alpha}{2} + \sin 2/\alpha \sin 1/\alpha\right] - 4\alpha\nu \cos 2/\alpha \sin 1/\alpha$$
$$+ 2[-2 \sin 2/\alpha \sin 1/\alpha + \ln \tan 3/\alpha - \ln \tan 1/2\alpha] , \qquad (7.24)$$

$$S^{u\,u}_{1\,2} = -\alpha^2 \sin 2/\alpha \sin 1/\alpha - 2\alpha\nu \cos 2/\alpha \sin 1/\alpha , \qquad (7.25)$$

$$S^{u\,w}_{1\,0} = \alpha(1+\nu)(1 - \cos 1/\alpha) , \qquad (7.26)$$

$$S^{u\,w}_{1\,1} = -2\alpha(1+\nu) \sin 2/\alpha \sin 1/\alpha + 4(1+\nu) \cos 2/\alpha \sin 1/\alpha . \qquad (7.27)$$

The coefficients of the u_k equations are given by the general expressions for $k = 2, 3, \ldots, N-3, N-2$ where

$$S^{u\,u}_{k\,k} = \alpha^2\left[\sin\frac{2k}{\alpha} + \sin\frac{2(k-1)}{\alpha}\right] \sin 1/\alpha - 4\alpha\nu \cos\frac{2k}{\alpha} \sin 1/\alpha$$
$$+ 2[-2 \sin\frac{2k}{\alpha} \sin 1/\alpha + \ln \tan\frac{2k+1}{2\alpha} - \ln \tan\frac{2k-1}{2\alpha}] , \qquad (7.28)$$

$$S^{u\,u}_{k\,k+1} = -\alpha^2 \sin\frac{2k}{\alpha}\sin 1/\alpha + 2\alpha\nu\cos\frac{2k}{\alpha}\sin 1/\alpha \,, \tag{7.29}$$

$$S^{u\,w}_{k\,k-1} = 2\alpha(1+\nu)\sin\frac{2(k-1)}{\alpha}\sin 1/\alpha \,, \tag{7.30}$$

$$S^{u\,w}_{k\,k} = -2\alpha(1+\nu)\sin\frac{2k}{\alpha}\sin 1/\alpha + 4(1+\nu)\cos\frac{2k}{\alpha}\sin 1/\alpha \,. \tag{7.31}$$

For the u_{N-1} and u_N equations, one has

$$S^{u\,u}_{N-1\,N-1} = \alpha^2\left[\sin\frac{2(N-2)}{\alpha} + \sin\frac{2(N-1)}{\alpha}\right]\sin 1/\alpha + \frac{\alpha^2}{2}\left[\sin\bar{\theta}\sin 1/\alpha - (1-\cos 1/\alpha)\cos\bar{\theta}\right] - 4\alpha\nu\cos\frac{2(N-1)}{\alpha}\sin 1/\alpha + 2\left[-2\sin\frac{2(N-1)}{\alpha}\sin 1/\alpha + \ln\tan\frac{2N-1}{2\alpha} - \ln\tan\frac{2N-3}{2\alpha}\right] \,, \tag{7.32}$$

$$S^{u\,u}_{N-1\,N} = -\alpha^2\sin\frac{2(N-1)}{\alpha}\sin 1/\alpha + 2\alpha\nu\cos\frac{2(N-1)}{\alpha}\sin 1/\alpha + \left[\frac{\alpha^2}{2} + \alpha(1+\nu\tan\bar{\theta}\right]\left[(1-\cos 1/\alpha)\cos\bar{\theta} - \sin\bar{\theta}\sin 1/\alpha\right] - \alpha\nu\left[\cos\bar{\theta}\sin 1/\alpha + (1-\cos 1/\alpha)\sin\bar{\theta}\right] \,, \tag{7.33}$$

$$S^{u\,w}_{N-1\,N-2} = 2\alpha(1+\nu)\sin\frac{2(N-2)}{\alpha}\sin 1/\alpha \,, \tag{7.34}$$

$$S^{u\,w}_{N-1\,N-1} = -2\alpha(1+\nu)\sin\frac{2(N-1)}{\alpha}\sin 1/\alpha + 4(1+\nu)\cos\frac{2(N-1)}{\alpha}\sin 1/\alpha \,, \tag{7.35}$$

$$S^{uu}_{NN} = \alpha^2 \sin\frac{2(N-1)}{\alpha}\sin 1/\alpha + [\frac{\alpha^2}{2} + 2(1+\nu)(\alpha + 2\tan\bar{\theta})\tan\bar{\theta}]$$

$$[\sin\bar{\theta}\sin 1/\alpha - (1-\cos 1/\alpha)\cos\bar{\theta}] + 2[\alpha\nu + 2(1+\nu)\tan\bar{\theta}]$$

$$[\cos\bar{\theta}\sin 1/\alpha + (1-\cos 1/\alpha)\sin\bar{\theta}] + 2[(1-\cos 1/\alpha)\cos\bar{\theta}$$

$$- \sin\bar{\theta}\sin 1/\alpha + \ln\tan\bar{\theta}/2 - \ln\tan\frac{2N-1}{2\alpha}]$$

$$+ \frac{1}{12}(\frac{h_s}{a_s})^2\{\frac{\alpha^2}{2}\tan^2\bar{\theta}[(\alpha-\nu\cot\bar{\theta})^2 - 2\alpha(\alpha-\nu\cot\bar{\theta}) + \alpha^2]$$

$$[\sin\bar{\theta}\sin 1/\alpha - (1-\cos 1/\alpha)\cos\bar{\theta}] - \alpha^2\nu^3\tan\bar{\theta}[\cos\bar{\theta}\sin 1/\alpha$$

$$+ (1-\cos 1/\alpha)\sin\bar{\theta}] + \frac{\alpha^2}{2}\tan^2\bar{\theta}[(1-\cos 1/\alpha)\cos\bar{\theta} - \sin\bar{\theta}\sin 1/\alpha$$

$$+ \ln\tan\frac{\bar{\theta}}{2} - \ln\tan\frac{2N-1}{2\alpha}] + \frac{\alpha^4}{4}\tan^2\bar{\theta}\sin\frac{2(N-1)}{\alpha}\sin 1/\alpha$$

$$+ \alpha^3\nu^2\tan^2\bar{\theta}\cos\frac{2(N-1)}{\alpha}\sin 1/\alpha + \frac{\alpha^2}{2}\tan^2\bar{\theta}[-2\sin\frac{2(N-1)}{\alpha}\sin 1/\alpha$$

$$+ \ln\tan\frac{2N-1}{2\alpha} - \ln\tan\frac{2N-3}{2\alpha}]\}\,, \qquad (7.36)$$

$$S^{uw}_{N\,N-2} = \frac{1}{12}(\frac{h_s}{a_s})^2\{\frac{\alpha^4}{4}\sin\frac{2(N-1)}{\alpha} + \frac{\alpha^3\nu^2}{2}\cos\frac{2(N-1)}{\alpha}\}\sin 1/\alpha\tan\bar{\theta}, \qquad (7.37)$$

$$S^{uw}_{N\,N-1} = 2\alpha(1+\nu)\sin\frac{2(N-1)}{\alpha}\sin 1/\alpha + \frac{1}{12}\left(\frac{h_s}{a_s}\right)^2\{\frac{\alpha^2}{4}\tan\bar{\theta}\,[(\alpha$$

$$- \nu\cot\bar{\theta})(\alpha - 2\nu\cot\bar{\theta}) - \alpha(2\alpha - 3\nu\cot\bar{\theta}) + \alpha^2]$$

$$[(1 - \cos 1/\alpha)\cos\bar{\theta} - \sin\bar{\theta}\sin 1/\alpha] + \alpha^2\nu^3[\cos\bar{\theta}\sin 1/\alpha$$

$$+ (1 - \cos 1/\alpha)\sin\bar{\theta}] - \frac{\alpha^2}{2}\tan\bar{\theta}[(1 - \cos 1/\alpha)\cos\bar{\theta} - \sin\bar{\theta}\sin 1/\alpha$$

$$+ \ln\tan\frac{\bar{\theta}}{2} - \ln\tan\frac{2N-1}{2\alpha}] - \frac{\alpha^4}{2}\tan\bar{\theta}\sin\frac{2(N-1)}{\alpha}\sin 1/\alpha$$

$$- \frac{3\alpha^3\nu^2}{2}\tan\bar{\theta}\cos\frac{2(N-1)}{\alpha}\sin 1/\alpha - \frac{\alpha^2}{2}\tan\bar{\theta}[-2\sin\frac{2(N-1)}{\alpha}\sin 1/\alpha$$

$$+ \ln\tan\frac{2N-1}{\alpha} - \ln\tan\frac{2N-3}{2\alpha}]\} \quad . \tag{7.38}$$

The coefficients of the w_0, w_1, and w_2 equations are given as the following:

$$S^{ww}_{0\,0} = 4(1+\nu)(1 - \cos 1/\alpha) + \frac{1}{12}\left(\frac{h_s}{a_s}\right)^2\{\frac{\alpha^4}{8}[(1 - \cos 1/\alpha)$$

$$+ 2\sin 2/\alpha\sin 1/\alpha]\} \quad , \tag{7.39}$$

$$S^{ww}_{0\,1} = -\frac{1}{12}\left(\frac{h_s}{a_s}\right)^2\{\frac{\alpha^4}{4}[(1 - \cos 1/\alpha) + 2\sin 2/\alpha\sin 1/\alpha]$$

$$+ \frac{\alpha^3\nu^2}{2}\cos 2/\alpha\sin 1/\alpha\} \quad , \tag{7.40}$$

$$S^{ww}_{0\,2} = \frac{1}{12}\left(\frac{h_s}{a_s}\right)^2\{\frac{\alpha^4}{8}[(1 - \cos 1/\alpha) + 2\sin 2/\alpha\sin 1/\alpha]$$

$$+ \frac{\alpha^3\nu^2}{2}\cos 2/\alpha\sin 1/\alpha\} \quad , \tag{7.41}$$

$$S_{1\,1}^{ww} = 8(1+\nu)\sin 2/\alpha \sin 1/\alpha + \frac{1}{12}\left(\frac{h_s}{a_s}\right)^2 \{ \frac{\alpha^4}{4} [2(1 - \cos 1/\alpha) + (4\sin 2/\alpha + \sin 4/\alpha)\sin 1/\alpha] + 2\alpha^3\nu^2 \cos 2/\alpha \sin 1/\alpha + \frac{\alpha^2}{2}[-2\sin 2/\alpha \sin 1/\alpha + \ln\tan 3/2\alpha - \ln\tan\frac{1}{2\alpha}]\} , \quad (7.42)$$

$$S_{1\,2}^{ww} = -\frac{1}{12}\left(\frac{h_s}{a_s}\right)^2 \{ \frac{\alpha^4}{4}[(1 - \cos 1/\alpha) + 2(\sin 2/\alpha + \sin 4/\alpha)\sin 1/\alpha] + \frac{\alpha^3\nu^2}{2}[3\cos 2/\alpha + \cos 4/\alpha]\sin 1/\alpha + \frac{\alpha^2}{2}[-2\sin 2/\alpha \sin 1/\alpha + \ln\tan 3/2\alpha - \ln\tan 1/2\alpha]\} , \quad (7.43)$$

$$S_{1\,3}^{ww} = \frac{1}{12}\left(\frac{h_s}{a_s}\right)^2 \{ \frac{\alpha^4}{4}\sin 4/\alpha \sin 1/\alpha + \frac{\alpha^3\nu^2}{2}\cos 4/\alpha \sin 1/\alpha\} , \quad (7.44)$$

$$S_{2\,2}^{ww} = 2(1+\nu)\sin 4/\alpha \sin 1/\alpha + \frac{1}{12}\left(\frac{h_s}{a_s}\right)^2 \{ \frac{\alpha^4}{8}[(1 - \cos 1/\alpha) + 2(\sin 2/\alpha + 4\sin 4/\alpha + \sin 6/\alpha)\sin 1/\alpha] + \alpha^3\nu^2[\cos 2/\alpha + 2\cos 4/\alpha]\sin 1/\alpha + \frac{\alpha^2}{2}[-2(\sin 2/\alpha + \sin 4/\alpha)\sin 1/\alpha + \ln\tan\frac{5}{2\alpha} - \ln\tan\frac{1}{2\alpha}]\} , \quad (7.45)$$

$$S_{2\,3}^{ww} = -\frac{1}{12}\left(\frac{h_s}{a_s}\right)^2 \{ \frac{\alpha^4}{2}[\sin 4/\alpha + \sin 6/\alpha]\sin 1/\alpha + \frac{\alpha^3\nu^2}{2}[3\cos 4/\alpha + \cos 6/\alpha]\sin 1/\alpha + \frac{\alpha^2}{2}[-2\sin 4/\alpha \sin 1/\alpha + \ln\tan\frac{5}{2\alpha} - \ln\tan\frac{3}{2\alpha}]\} , \quad (7.46)$$

$$S_{2\,4}^{ww} = \frac{1}{12}\left(\frac{h_s}{a_s}\right)^2 [\frac{\alpha^4}{4}\sin 6/\alpha + \frac{\alpha^3\nu^2}{2}\cos 6/\alpha]\sin 1/\alpha . \quad (7.47)$$

The general expressions where k = 3, 4, ..., N-4, N-3 are

$$S^{ww}_{kk} = 8(1+\nu)\sin\frac{2k}{\alpha}\sin 1/\alpha + \frac{1}{12}\left(\frac{h_s}{a_s}\right)^2 \{ \frac{\alpha^4}{4} [\sin\frac{2(k-1)}{\alpha} + \sin\frac{2(k+1)}{\alpha}] \sin 1/\alpha + \alpha^3\nu^2 [\cos\frac{2(k-1)}{\alpha} + 2\cos\frac{2k}{\alpha}] \sin 1/\alpha + \frac{\alpha^2}{2} [-2(\sin\frac{2(k-1)}{\alpha} + \sin\frac{2k}{\alpha}) \sin 1/\alpha + \ln\tan\frac{2k+1}{2\alpha} - \ln\tan\frac{2k-3}{2\alpha}]\} , \quad (7.48)$$

$$S^{ww}_{k\,k+1} = -\frac{1}{12}\left(\frac{h_s}{a_s}\right)^2 \{\frac{\alpha^4}{2} [\sin\frac{2k}{\alpha} + \sin\frac{2(k+1)}{\alpha}] \sin 1/\alpha + \frac{\alpha^3\nu^2}{2} [3\cos\frac{2k}{\alpha} + \cos\frac{2(k+1)}{\alpha}] \sin 1/\alpha + \frac{\alpha^2}{2} [-2\sin\frac{2k}{\alpha}\sin 1/\alpha + \ln\tan\frac{2k+1}{2\alpha} - \ln\tan\frac{2k-1}{2\alpha}]\} , \quad (7.49)$$

$$S^{ww}_{k\,k+2} = \frac{1}{12}\left(\frac{h_s}{a_s}\right)^2 [\frac{\alpha^4}{4}\sin\frac{2(k+1)}{\alpha} + \frac{\alpha^3\nu^2}{2}\cos\frac{2(k+1)}{\alpha}] \sin 1/\alpha . \quad (7.50)$$

For u_{N-2} and u_{N-1}, one has

$$S^{ww}_{N-2\,N-2} = 8(1+\nu)\sin\frac{2(N-2)}{\alpha}\sin 1/\alpha + \frac{1}{12}\left(\frac{h_s}{a_s}\right)^2 \{ \frac{\alpha^4}{4} [\sin\frac{2(N-3)}{\alpha} + 4\sin\frac{2(N-2)}{\alpha} + \sin\frac{2(N-1)}{\alpha}] \sin 1/\alpha + \alpha^3\nu^2 [\cos\frac{2(N-3)}{\alpha} + 2\cos\frac{2(N-2)}{\alpha}] \sin 1/\alpha + \frac{\alpha^2}{2} [-2(\sin\frac{2(N-3)}{\alpha} + \sin\frac{2(N-2)}{\alpha}) \sin 1/\alpha + \ln\tan\frac{2N-3}{2\alpha} - \ln\tan\frac{2N-7}{2\alpha}] \} , \quad (7.51)$$

$$S^{w}_{N-2\,N-1} = -\frac{1}{12}\left(\frac{h_s}{a_s}\right)^2 \left\{ \frac{\alpha^4}{2}\left[\sin\frac{2(N-2)}{\alpha} + \sin\frac{2(N-1)}{\alpha}\right]\sin 1/\alpha \right.$$

$$+ \frac{\alpha^3\nu^2}{2}\left[3\cos\frac{2(N-2)}{\alpha} + \cos\frac{2(N-1)}{\alpha}\right]\sin 1/\alpha$$

$$\left. + \frac{\alpha^2}{2}\left[-2\sin\frac{2(N-2)}{\alpha}\sin 1/\alpha + \ln\tan\frac{2N-3}{2\alpha} - \ln\tan\frac{2N-5}{2\alpha}\right] \right\},$$

(7.52)

$$S^{w}_{N-1\,N-1} = 8(1+\nu)\sin\frac{2(N-1)}{\alpha}\sin 1/\alpha + \frac{1}{12}\left(\frac{h_s}{a_s}\right)^2 \left\{ \frac{\alpha^4}{4}\left[\sin\frac{2(N-2)}{\alpha}\right.\right.$$

$$\left. + 4\sin\frac{2(N-1)}{\alpha}\right]\sin 1/\alpha + \frac{\alpha^2}{8}\left[(\alpha - 2\nu\cot\bar{\theta})^2 + \alpha^2\right.$$

$$\left. - 2\alpha(\alpha - 2\nu\cot\bar{\theta})\right]\left[\sin\bar{\theta}\sin 1/\alpha - (1-\cos 1/\alpha)\cos\bar{\theta}\right]$$

$$+ \alpha^3\nu^2\left[\cos\frac{2(N-2)}{\alpha} + 2\cos\frac{2(N-1)}{\alpha}\right]\sin 1/\alpha - \alpha^2\nu^3\cot\bar{\theta}\left[\cos\bar{\theta}\sin 1/\alpha\right.$$

$$\left. + (1-\cos 1/\alpha)\sin\bar{\theta}\right] + \frac{\alpha^2}{2}\left[-2\sin\frac{2(N-2)}{\alpha}\sin 1/\alpha + \ln\tan\frac{2N-3}{2\alpha}\right.$$

$$\left. - \ln\tan\frac{2N-5}{2\alpha}\right] + \frac{\alpha^2}{2}\left[-2\sin\frac{2(N-1)}{\alpha}\sin 1/\alpha + \ln\tan\frac{2N-1}{2\alpha}\right.$$

$$\left. - \ln\tan\frac{2N-3}{2\alpha}\right] + \frac{\alpha^2}{2}\left[(1-\cos 1/\alpha)\cos\bar{\theta} - \sin\bar{\theta}\sin 1/\alpha\right.$$

$$\left. + \ln\tan\frac{\bar{\theta}}{2} - \ln\tan\frac{2N-1}{2\alpha}\right] \right\}. \qquad (7.53)$$

7.3 List of Symbols

a_d = radius of piezoelectric disk

a_s = radius of shell

b_r = scalar modal participation factor

D_i = electric displacement vector

d_{mij} = piezoelectric strain constant

E_i = electric field intensity vector

F = force per unit circumferential length

f_i = body forces per unit volume

h_d = thickness of piezoelectric disk

h_s = thickness of shell

I_o = amplitude of steady state electrical current

i = electrical current

$J_N(x)$ = Bessel function of first kind of order N

k_p = planar coupling coefficient

L = Lagrangian energy

M_N = mobility at lower edge of shell (j = N)

M_N^* = specific mobility at lower edge of shell (j = N)

M_θ = moment per unit length acting in θ-direction

M_φ = moment per unit length acting in φ-direction

N_θ = mid-plane force per unit length acting in θ-direction

N_φ = mid-plane force per unit length acting in φ-direction

$\{p\}$ = column vector of external forces

p^* = amplitude of steady state external forcing function

Q = electrical charge

Q_T = amplitude of steady state electrical charge

q = general displacement

q^* = amplitude of general displacements for steady state motion

$\{q\}$ = column vector of displacement

R_r = normalizing factor

$[S]$ = stiffness matrix

S_{ij} = strain tensor

$S_{ij}^{k\ell}$ = stiffness coefficient in stiffness matrix [S]

$S_{ijk\ell}^{E}$ = elastic compliance matrix at constant electric field

T = kinetic energy

T_{ij} = stress tensor

t = time

U_1 = strain energy due to stretching

U_2 = strain energy due to bending

U_r = amplitude of steady state displacement of disk

U_{ext} = strain energy due to external forces per unit area

u,v,w = displacement components of spherical cap with respect to r, φ, θ directions respectively

u^*,w^* = amplitude of displacements for steady state motion

u_i = displacement in the i^{th} direction

V = potential energy

V_o = steady state voltage amplitude

V_p = potential energy per unit volume

$\bar{X},\bar{Y},\bar{Z}$ = external forces per unit area acting on spherical cap

X,Z = external forces per unit area other than inertia forces

Y = electrical admittance

Y^E = Young's Modulus for a constant electric field

$Y_N(x)$ = Bessel function of second kind of order N

Z = electrical impedance

Z' = arbitrary specific impedance on boundary of disk

Z_N = impedance at lower edge of shell (j = N)

Z_N^* = specific impedance at lower edge of shell (j = N)

α = inverse of half-angle increment

Γ = imaginary part of specific impedance on boundary of disk

$\Delta\theta$ = half-angle increment

δ_{ij} = Kronecker delta

ϵ_{nm}^T = permittivity matrix at constant stress

θ_T = absolute temperature

$\bar{\theta}$ = opening angle of spherical cap

λ_r = r^{th} eigenvalue

μ = shear modulus of shell material

ρ = density

σ = Poisson's ratio

σ^* = entropy per unit volume

$\{\varphi_r\}$ = eigenvector corresponding to λ_r eigenvalue

Ω = real part of specific impedance on boundary of disk

ω = angular velocity

Unclassified
Security Classification

DOCUMENT CONTROL DATA - R & D

(Security classification of title, body of abstract and indexing annotation must be entered when the overall report is classified)

ORIGINATING ACTIVITY (Corporate author)
Center for Acoustical Studies
Department of Mechanical & Aerospace Engineering
N. C. State University, Raleigh, N. C. 27607

2a. REPORT SECURITY CLASSIFICATION
Unclassified

2b. GROUP

REPORT TITLE
A Mathematical Model for the Class V Flextensional Underwater Acoustic Transducer

DESCRIPTIVE NOTES (Type of report and inclusive dates)
Technical Report, 1970

AUTHOR(S) (First name, middle initial, last name)
Nelson, Ralph A., Jr. and Royster, Larry H.

REPORT DATE	7a. TOTAL NO. OF PAGES	7b. NO. OF REFS
January 1970	81	24

CONTRACT OR GRANT NO.	9a. ORIGINATOR'S REPORT NUMBER(S)
Nonr 486(11)	Technical Report No. 12
PROJECT NO. NR 185-551	9b. OTHER REPORT NO(S) (Any other numbers that may be assigned this report) CAS-57

DISTRIBUTION STATEMENT
Distribution of this document is unlimited.

SUPPLEMENTARY NOTES	12. SPONSORING MILITARY ACTIVITY
	Office of Naval Research, Acoustic Programs and the Naval Underwater Sound Laboratory

ABSTRACT

The purpose of this investigation is to develop a mathematical model for the Class V flextensional underwater acoustic transducer.

The transducer is approximated through the consideration of three distinct problems. The problem of a thin piezoelectric disk with an arbitrary impedance on its edge is solved in terms of Bessel functions. The shell vibration problem is solved using a finite difference model to approximate the shell. The acoustic radiation problem is solved by obtaining the source density distribution for a system of quadrilaterals representing the transducer. With the source density of each quadrilateral, the near and far field pressures and velocities can be found. Utilizing these three components, a model is then constructed for the transducer.

A comparison of the results from the mathematical model with those obtained from experiments is made in order to validate the model.

14 KEY WORDS	LINK A		LINK B		LINK C	
	ROLE	WT	ROLE	WT	ROLE	WT
Flextensional transducer Class V Shell Vibration-Guided on Boundaries Acoustic Radiation Piezoelectric circular disk arbitrary impedance on boundary						